Differential Roles of Ventral Pallidum Subregions During Cocaine Self-Administration Behaviors

David H. Root, Sisi Ma, David J. Barker, Laura Megehee, Brendan M. Striano, Carla M. Ralston, Anthony T. Fabbricatore, and Mark O. West*

Department of Psychology, Rutgers University, New Brunswick, New Jersey 08903

ABSTRACT

The ventral pallidum (VP) is necessary for drug-seeking behavior. VP contains ventromedial (VPvm) and dorsolateral (VPdl) subregions, which receive projections from the nucleus accumbens shell and core, respectively. To date no study has investigated the behavioral functions of the VPdl and VPvm subregions. To address this issue, we investigated whether changes in firing rate (FR) differed between VP subregions during four events: approaching toward, responding on, or retreating away from a cocaine-reinforced operandum and a cocaine-associated cue. Baseline FR and waveform characteristics did not differ between subregions. VPdl neurons exhibited a greater change in FR compared with VPvm neurons during approaches toward, as well as responses on, the cocaine-reinforced operandum. VPdl neurons were more likely to exhibit a similar change in FR (direction and magnitude) during approach and response than VPvm neurons. In contrast, VPvm firing patterns were heterogeneous, changing FRs during approach or response alone, or both. VP neurons did not discriminate cued behaviors from uncued behaviors. No differences were found between subregions during the retreat, and no VP neurons exhibited patterned changes in FR in response to the cocaine-associated cue. The stronger, sustained FR changes of VPdl neurons during approach and response may implicate VPdl in the processing of drug-seeking and drug-taking behavior via projections to subthalamic nucleus and substantia nigra pars reticulata. In contrast, the heterogeneous firing patterns of VPvm neurons may implicate VPvm in facilitating mesocortical structures with information related to the sequence of behaviors predicting cocaine self-infusions via projections to mediodorsal thalamus and ventral tegmental area. J. Comp. Neurol. 521:558–588, 2013.

INDEXING TERMS: striatum; accumbens; striatopallidum; dopamine; pallidum

First conceptualized by Heimer and colleagues (Heimer and Wilson, 1975; Heimer, 1978), the ventral pallidum (VP) was hypothesized to be a primary participant in the neuronal control of motivated behaviors (Mogenson et al., 1980). Over 30 subsequent years of research, the VP has been shown to be critical for natural reward-seeking and drug-seeking behaviors. In rodent models of drug seeking, VP lesions or pharmacological challenges block morphine-induced sensitization (Johnson and Napier, 2000; Mickiewicz et al., 2009), drug-induced conditioned place preference (Gong et al., 1997; Rademacher et al., 2006; Dallimore et al., 2006), self-administration (Robledo and Koob, 1993), and reinstatement (McFarland and Kalivas, 2001; McFarland et al., 2004; Tang et al., 2005). In humans, postmortem analyses from cocaine abusers have shown alterations in VP neuropeptide expression (Frankel et al., 2008). However, akin to its primary afferent, the nucleus accumbens (NAcc), the VP contains two "neurochemically distinct subterritories" that differ in their projection patterns (Zahm et al., 1996) and likely exhibit differential roles in drug-seeking behavior. Whether they do so remains untested and is the subject of the present investigation.

The entire VP is characterized by dense substance P-immunoreactive fibers (Haber and Nauta, 1983;

Additional Supporting Information may be found in the online version of this article.

David H. Root's current address is Neuronal Networks Section, Integrative Neuroscience Research Branch, National Institute on Drug Abuse, 251 Bayview Blvd., Baltimore, MD 21224

Grant sponsor: National Institute on Drug Abuse; Grant number: DA 006886; Grant number: DA 026252; Grant number: DA 029873.

*CORRESPONDENCE TO: Mark O. West, PhD, Department of Psychology, Rutgers University, 152 Frelinghuysen Road, New Brunswick, NJ 08854. E-mail: markwest@rutgers.edu

Received February 2, 2012; Revised April 30, 2012; Accepted July 9, 2012

DOI 10.1002/cne.23191

Published online July 18, 2012 in Wiley Online Library (wileyonlinelibrary.com)

Groenewegen and Russchen, 1984; Haber et al., 1985, 1990; Zahm and Heimer, 1988, 1990; Zahm, 1989; Heimer et al., 1991; Groenewegen et al., 1993; Kuo and Chang, 1992; Kalivas et al., 1993; Zahm et al., 1996). The ventromedial subregion (VPvm) is demarcated by dense neurotensin-immunoreactive fibers and a lack of calbindin-d28k immunoreactivity (Zahm and Heimer, 1988, 1990; Zahm, 1989; Zahm et al., 1996; Geisler and Zahm, 2006a). Conversely, the dorsolateral subregion (VPdl) is distinguished by dense calbindin-d28k-immunoreactive fibers and a lack of neurotensin immunoreactivity (Zahm et al., 1996; Riedel et al., 2002; Tripathi et al., 2010).

In addition to their distinct immunoreactivities, VPvm and VPdl subregions participate in independent neuronal circuits. The neurotensin-immunoreactive VPvm receives projections from the NAcc shell and projects predominantly to the mediodorsal thalamus (MDT) and ventral tegmental area (VTA; Zahm and Heimer, 1988, 1990; Zahm, 1989; Heimer et al., 1991; Zahm and Brog, 1992; Groenewegen et al., 1993; Kuroda and Price, 1991; Kalivas et al., 1993; Zahm et al., 1996; Churchill et al., 1996; O'Donnell et al., 1997; Tripathi et al., 2010). In contrast, the calbindin-d28k-immunoreactive VPdl receives projections from the NAcc core (which exhibits selective calbindin-d28k immunoreactivity compared with the shell [Zahm and Brog, 1992]) and projects predominantly to the substantia nigra pars reticulata and subthalamic nucleus but weakly to MDT (Zahm and Heimer, 1990; Groenewegen et al., 1993; Bell et al., 1995; Zahm et al., 1996; O'Donnell et al., 1997; Tripathi et al., 2010).

The discrete projection patterns of VPvm and VPdl suggest that the VP subregions differentially process behaviors within the ventral striatopallidal circuit. To the best of our knowledge, no study has examined whether these subregions exhibit differential behavioral functions. The present study recorded single units during cocaine self-administration from the VPvm and VPdl, as delineated by substance P, calbindin-d28k, and neurotensin immunohistochemistry. First, we extend our preliminary characterization of VP single units during cocaine self-administration (Root et al., 2010) by determining which behaviors were coincident with changes in firing rate (FR) during self-administration. Second, we examined whether changes in FR during distinct cocaine-seeking behaviors differed between VP subregions.

NAcc neurons exhibit changes in FR during distinct components of drug-seeking behaviors, including approaching and responding on a cocaine-reinforced lever (Chang et al., 1994, 1997, 2000). However, in our experience with a cocaine-reinforced lever press, rats often exhibit a uniform ambulatory behavior that obscures both offset of approach and onset of response, as well as offset of response and onset of retreat. Therefore, we utilized a well-characterized long-distance vertical head movement as the operant (Pederson et al., 1997; Tang et al., 2007; Pawlak et al., 2010; Root et al., 2011), which allowed us to discriminate onsets and offsets of approach, response, and retreat behaviors during self-administration. Specifically, the placement of the operandum within the corner of the self-administration chamber precluded locomotion during the operant response (i.e., alternating limb movements; Root et al., 2011). In contrast, the preceding approach toward and subsequent retreat away from the operandum involved turning and ambulatory behaviors.

Prior subregional examinations of NAcc neurons during cocaine self-adminstration revealed that NAcc core neurons exhibit greater changes in FR than neurons in the medial NAcc shell over two time periods: 1) prior to response completion and 2) following response completion (Ghitza et al., 2004, 2006; Hollander and Carelli, 2005; Fabbricatore et al., 2010). The epoch "prior to response completion" consists of two distinct behaviors, approaching toward and responding on the operandum, whereas the epoch "following response completion" partially consists of retreating away from the operandum. By utilizing the vertical head movement operant, we distinguished changes in FR during approaches toward the operandum, responses on the operandum, and retreats away from the operandum. To investigate functional compartmentalization in the VP, we analyzed whether changes in FR during approach, response, or retreat alone, as well as correlations between two of these behaviors' changes in FR, differed between VP subregions. Given that the NAcc core projects to the VPdl, whereas the NAcc shell projects to the VPvm, it was predicted that VPdl neurons would exhibit greater changes in FR than VPvm neurons during approach and response (i.e., prior to response completion) as well as retreat behaviors (i.e., following response completion).

MATERIALS AND METHODS

Subjects and surgery

Male Long-Evans rats (n = 25; 320–340 g; Charles River, Wilmington, MA) were anesthetized with sodium pentobarbital (approximately 50 mg/kg, i.p.). Prior to surgery, the rats received injections of atropine methylnitrate (10 mg/kg, i.p.) and penicillin G (75,000 U/0.25 ml, i.m.) to reduce the risk of pulmonary edema and bacterial infection, respectively. To block postsurgical pain sensitivity, animals were injected subcutaneously with 0.25 ml bupivacaine HCl (0.25%; Abbott Laboratories, North Chicago, IL) spread over eight injection sites of the incisions on the head and neck. Anesthesia was maintained with periodic i.p. injections of ketamine HCl (approximately 60

mg/kg, i.p.) and sodium pentobarbital (approximately 15 mg/kg, i.p.). After catheter implantation into the right jugular vein, a pair of 2 × 4 arrays (Microwire Technologies, Heightstown, NJ) composed of Quad Teflon-coated stainless-steel microwire electrodes (California Fine Wire, Grover Beach, CA) was implanted bilaterally into the VP (between 0.7 and −0.9 AP, ±0.8 and ±3.1 ML, −8.0 DV; Paxinos and Watson, 1997) and secured with dental cement. The diameter of each uninsulated microwire tip was 50 μm, and wires were separated by 300–400 μm (center–center). An insulated 0.01-in. ground wire, stripped 5 mm from the tip, was implanted 5.5 mm ventral from the skull. The microconnector strip (Omnetics, Minneapolis, MN) was oriented mediolaterally (ear to ear), anterior to the interaural line, which prevented the harness cabling from breaking photocells during the task. After surgery, rats were individually housed with access to food and water in the cocaine self-administration chambers to recover for at least 1 week. Animals lived in the self-administration chambers and were maintained at 320–350 g body weight with ad libitum access to water and approximately 12–24 g lab chow (Rat Diet No. 5012; Purina Mills Nutrition International, St. Louis, MO) following daily self-administration sessions. Rats received infusions of heparinized saline every 25 minutes, except during self-administration sessions to preserve catheter patency. Protocols were performed in compliance with the *Guide for the care and use of laboratory animals* (NIH Publication 865-23) and were approved by the Institutional Animal Care and Use Committee, Rutgers University.

Electrophysiological procedures

Sixteen neural signals were led through four quad-channel operational amplifiers (TLC2264; Texas Instruments, Dallas, TX) inside a custom-made recording harness (MB Turnkey Designs, Hillsborough, NJ) and fluid/electronic swivel (CAY-675-24, Airflyte Electronics, Bayonne, NJ) to a preamplifier (MB Turnkey Designs) that differentially amplified (×10) the signal on the recording electrode against another microwire that did not exhibit a single unit. The signal was then bandpass filtered (450 Hz to 10 kHz; roll off 1.5 dB/octave at 1 kHz and −6 dB/octave at 11 kHz) and amplified ×700 between rollovers (MB Turnkey Designs). With software and hardware from DataWave Technologies, electrical signals were sampled (50 kHz sampling frequency per wire) and stored for off-line analysis.

One recording of all microwires per animal occurred between days 14 and 24 of self-administration training. The rationale for recording at this time point was as follows. First, we have previously demonstrated rapid phasic changes in FR surrounding cocaine-reinforced responses during this period (Root et al., 2010). Second, this time point follows the development of escalated drug intake (Root et al., 2011), posited to exemplify "addiction-like behavior" in rats (Ahmed and Koob, 1998; Deroche-Gamonet et al., 2004). Third, well-trained animals quickly load to stable asymptotic drug levels that exhibit little variability during the recording session, mitigating pharmacological differences between responses (Root et al., 2011).

Isolation and separation of individual neural waveforms from background noise and waveforms of other neurons recorded from the same microwire were conducted post hoc using DataWave spike sorting and separation software. First, neural discharges were sorted by using waveform parameters, including principal components 1 and 2, valley voltage, peak voltage, voltages at user-defined time cursors, spike height, and peak voltage time. Scatterplots of any two waveform parameters were displayed in a window, with all windows' parameter combinations displayed on one screen simultaneously. Each point plotted on the scatterplot corresponded to one recorded waveform. Each cluster of dots represented similar waveforms and was separated from other clusters by enclosing it within an elliptical window. All waveforms of the putative individual neuron during the entire session (6–10 hours) were then replayed on a computer-simulated oscilloscope to assess the stability of neural waveforms. Waveforms whose parameters did not remain stable were discarded. Second, an interspike interval histogram was constructed. If discharges occurred within the first 2 msec in the interspike interval, corresponding to a neuron's natural refractory period, the recording was not considered that of a single neuron and was discarded. When more than a single population of neural waveforms appeared to have been recorded from a given wire, cross-correlation was used to confirm that the populations corresponded to distinct neurons. Specifically, if discharges occurred within the first 2 msec in the cross-correlation and both neurons contained 0 discharges within their interspike intervals, both neurons were considered independent single units. Neurons exhibiting signal-to-noise ratios less than 2:1 were discarded.

Head movement task

Long-distance vertical head movements were selected as the operant. First, this operant facilitates rapid shaping as well as the ability to characterize certain parameters of the movement during water or cocaine self-administration, as our laboratory has done previously (Pederson et al., 1997; Tang et al., 2007; Pawlak et al., 2010; Root et al., 2011). Second, with this operant, we have demonstrated the acquisition of skilled cocaine self-administration behavior (Root et al., 2011), as hypothesized to occur

in human drug users (Tiffany, 1990). Third, this apparatus measures operant movements and readily distinguishes them from any stereotypical (e.g., cocaine-induced) movements that occur at 10 Hz (Root et al., 2011; Fowler et al., 2003, 2007; see also Supp. Info. Movies 1 and 2). Such stereotypical movements are rarely emitted in the corner containing the apparatus.

The apparatus tracked vertical head movements with infrared-emitting diodes capable of transistor–transistor logic (HOA6299; Honeywell, Morristown, NJ). Six photocells were arranged along a 50° arc over 69 mm in one corner of the self-administration chamber. The lowest of six photocell beams, photocell 1, was positioned 13 mm above the floor. Photocell 6 was the highest photocell. For full apparatus details and several images see Root et al. (2011). For neuronal analysis during vertical head movements, time stamps of photocell beam breaks were collected by using a DataWave Technologies setup, which allowed a unique decimal code for simultaneous beam breaks (i.e., photocell beams 1 and 2 broken at the same time). Two simultaneous photocell beam breaks of consecutive photocells were considered as half steps, equally between two photocells. For example, simultaneously breaking photocells 2 and 3 was considered 2.5. For neuronal analyses during responses, movement onset was defined as a photocell beam break for which at least the next photocell beam break was 0.5, 1, or 1.5 larger than the previous photocell beam break and less than 1 second in duration from the original photocell beam break. Offset was defined as the last instance for which the previous photocell beam break was 0.5, 1, or 1.5 larger than the previous photocell beam break and less than 1 second in duration from the onset. For both behavioral and neuronal analyses, all photocell beam breaks were recorded for offline analysis of different movements (1 msec resolution). A criterion head movement was defined as a vertical head movement breaking photocells 2, 3, 4, and 5 consecutively within 1 second (schematized in Fig. 1B). The criterion head movement required at least a 43-mm movement (cf. Tang et al., 2007; Pawlak et al., 2010), which started at or below the second photocell beam and cross the fifth or sixth photocell.

Self-administration began daily with the onset of the house light. Self-administration sessions were controlled by custom programs written in MED-PC (MED-Associates, St. Albans, VT). At the beginning of the first day, vertical head movements in the "head movement corner" were shaped via delivery of cocaine infusion (0.24 mg/0.2 ml/7.5 seconds infusion) by the experimenter in the presence of a discriminative stimulus (S^D) tone (3.5 kHz, 70 dB). During acquisition, the S^D was sounded for 2 minutes or until a criterion head movement was made. If a criterion movement was made, three events occurred simultaneously: the S^D was terminated, cocaine delivery began, and a 40-second time-out period began. If a criterion movement was not made, the S^D was terminated after 2 minutes, and a 5-second timeout period began. The S^D was sounded again following the time-out period. Criterion movements within the time-out period were recorded but had no programmed consequence. Thus, the S^D set the occasion for each cocaine-reinforced movement, as in previous investigations of NAcc shell and core neurons during cocaine self-administration (Ghitza et al., 2004). Operant responses were readily shaped within the first

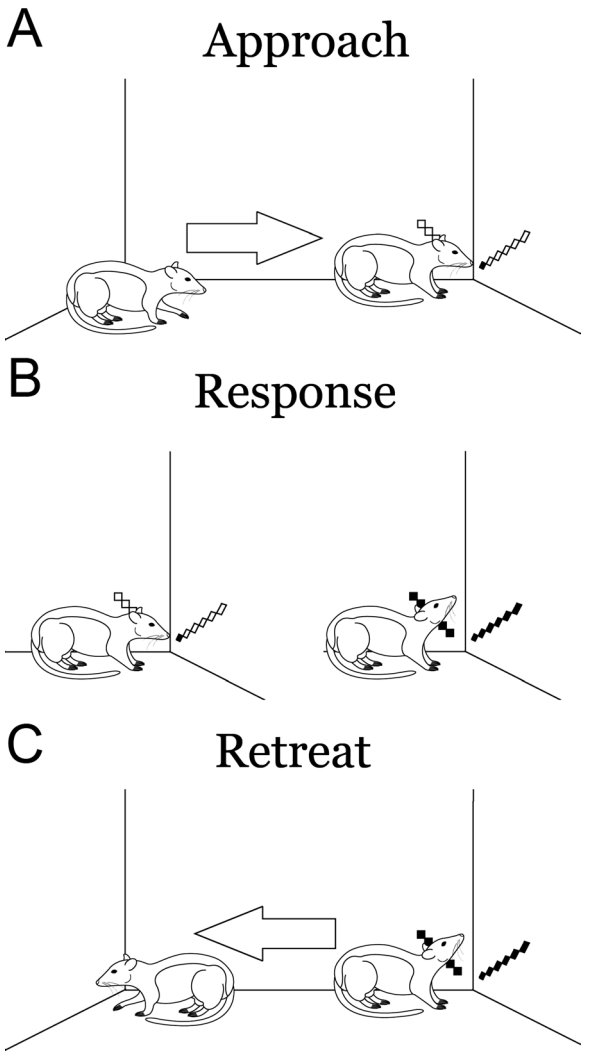

Figure 1. Behaviors schematized for neuronal analysis. Behaviors included the approach toward the photocell corner (**A**), criterion head movement operant response (**B**), and retreat away from the photocell corner (**C**). Arrows in A,C indicate locomotion that is absent from B. The criterion movement consisted of a vertical head movement breaking photocells 1 or 2 through 5 or 6, consecutively, under 1 second. In this example, the rat executes a vertical head movement breaking photocells 1–6.

day in most rats. The shaping process began with rewarding breaking photocell 2 for 10 rewards, then rewarding breaking photocells 2 and 3 consecutively within 1 second for five rewards. Shaping continued with rewarding breaking photocells 2, 3, and 4 consecutively within 1 second for five rewards and finally rewarding the final contingency of breaking photocells 2, 3, 4, and 5 within 1 second consecutively. Most rats self-administered at the final contingency for 2 additional days under the same S^D duration, infusion dose, time-out duration, and contingency.

After acquisition, starting typically on day 4, animals began normal training. Normal training consisted of the same fixed ratio 1 schedule of reinforcement during S^D presentations. To maximize the amount of time the animal spent at asymptotic drug levels where electrophysiological analyses occurred (see under Neuronal analysis section), prior to the tenth self-infusion, the S^D was sounded for 30 seconds and the time-out was fixed to 5 seconds. All subsequent time-outs and S^D durations were fixed to 30 seconds with a dose of 0.06 mg/0.05 ml/1.875 seconds to increase the number of events used in neuronal analyses. In all cases, when the rat satisfied the criteria for a criterion head movement while the S^D was sounded, three events occurred simultaneously: the S^D was terminated, cocaine delivery began, and the time-out began. If the rat did not execute a criterion head movement during S^D presentation, the S^D was terminated after 30 seconds and the time-out began. Criterion head movements that occurred when the S^D was not sounded (time-out) were recorded but had no programmed consequence. The present schedule of reinforcement allowed rats to attain a maximum instantaneous calculated drug level of 7.16 mg/kg, which was above the level self-administered by all rats. That is, each rat was able to self-administer its "preferred" level, or satiety threshold level, of drug (Root et al., 2011). During training, self-administration sessions ended after 6 hours had elapsed or 280 rewards had been earned, whichever occurred first. During the recording session, the self-administration session ended 6 hours following the tenth self-infusion of cocaine. Overnight between self-administration sessions, a rectangular 2 in. $\times$ 2 in. $\times$ 8 in. Plexiglas block was fastened into the head movement corner to block extinction learning. Rats were never "primed", i.e., noncontingently administered infusions of cocaine to initiate self-administration.

Histological procedures

At least 1 hour following the final self-administration session, animals were injected subcutaneously 18 hours and 4 hours prior to perfusion with 2 mg/kg of haloperidol to enhance subsequent immunohistochemical staining in the VP (Eggerman and Zahm, 1988; Zahm and Heimer, 1990; Geisler and Zahm, 2006a). At 0 hours, animals were anesthetized with an overdose of sodium pentobarbital (150–200 mg/kg, i.p.). Anodal current (50 μA for 3 second) was passed through each microwire to mark the tip location, and the animal was perfused with saline followed by 4% paraformaldehyde. The brain was removed and fixed in a solution of 4% paraformaldehyde overnight. Subsequently, the brain was stored in a 30% sucrose-phosphate buffer solution at 4°C. Brains were coronally sliced at a thickness of 40 μm through VP and placed in phosphate buffer-filled 10-ml net wells for immunohistochemistry.

All immunohistochemical steps were carried out under gentle agitation on a horizontal rotator (Laboratory-Line; Fisher, Pittsburgh, PA). Free-floating sections were rinsed in 0.1 M phosphate buffer (pH 7.4), placed into 1% sodium borohydride for 15 minutes, thoroughly rinsed in 0.1 M phosphate buffer again, pretreated with 0.1 M phosphate buffer containing 0.1% Triton X-100 and 3% normal goat serum for 1 hour, and then transferred into a solution containing a primary antibody, namely, polyclonal anti-neurotensin (ImmunoStar, Hudson, WI; formerly DiaSorin Histochemical as well as Incstar; catalog No. 20072) at a dilution of 1:6,500, polyclonal anti-calbindin-d28k (ImmunoStar; catalog No. 24427) at a dilution of 1:6,000, or polyclonal anti-substance P (ImmunoStar; catalog No. 20064) at 1:6,500 in 0.1 M phosphate buffer with 0.1% Triton X-100 and 3% normal goat serum overnight (see Table 1 and Antibody characterization section for details regarding the primary antibodies used). Every first of three sections was prepared with anti-substance P, every second of three sections was prepared with anti-calbindin-d28k, and every third of three sections was prepared with anti-neurotensin.

On the following day, after thorough rinsing in 0.1 M phosphate buffer with 0.1% Triton X-100, sections were placed in a solution containing biotinylated antibody against rabbit immunoglobulin (Vector, Burlingame, CA) at a dilution of 1:200 in 0.1 M phosphate buffer with 0.1% Triton X-100 for 1 hour. The sections were again rinsed in 0.1 M phosphate buffer with 0.1% Triton X-100 and immersed in a solution containing avidin-biotin-peroxidase complex (Vector; 1:200 in 0.1 M phosphate buffer containing 0.1% Triton X-100) for another 1 hour. After thorough rinsing in 0.1 M phosphate buffer, a color reaction was developed by immersing the sections for 6 minutes in a solution of 0.01 M phosphate buffer containing 0.05% 3,3′-diaminobenzidine and 0.003% hydrogen peroxide. Sections were mounted onto gelatin-coated slides and incubated in a solution of 5% potassium ferrocyanide and 10% HCl to stain the iron deposits left at the marked microwire recording tip. Sections were then

TABLE 1.
Primary Antibodies Used[1]

Antigen (what is being stained for)	Immunogen (against which the antibody was raised; full sequence and species)	Manufacturer, species in which antibody was raised; mono- vs. polyclonal, catalog or lot No.	Dilution used
Substance P	Synthetic substance P (RPKPQQFFGLM) coupled to keyhole limpet hemocyanin with carbodiimide	ImmunoStar (Hudson, WI), rabbit polyclonal, No. 20064	1:6,500
Calbindin-d28k	Calbindin-d28k purified from bovine cerebellum	ImmunoStar, rabbit polyclonal, No. 24427	1:6,000
Neurotensin	Synthetic peptide (human) neurotensin coupled to bovine thyroglobulin with glutaraldehyde	ImmunoStar, rabbit polyclonal, No. 20072	1:6,500

[1]For further details regarding the primary antibodies, see the Antibody characterization section.

dehydrated through a graded series of alcohol, transferred into xylene, and coverslipped with Permount (Fisher). Sections were photographed, and some photographs were then enhanced by using "Hard Light" blend mode in Photoshop CS6 (Adobe Systems, San Jose, CA).

Antibody characterization

The polyclonal anti-substance P antibody was raised in rabbit against synthetic substance P (RPKPQQFFGLM) coupled to keyhole limpet hemocyanin with carbodiimide and shows no cross-reactivity with other brain peptides, including neurokinin A, neurokinin B, somatostatin, and neuropeptide K. According to the manufacturer, specific immunostaining with the antibody was completely abolished by preadsorption with substance P at a final concentration of 10 μg/ml. Several other laboratories have also reported the abolition of specific immunostaining with the antibody by preadsorption with substance P (Brog et al., 1993; Zahm et al., 1996; Weissner et al., 2006; Cantwell and Cassone, 2006; Kim et al., 2008).

The polyclonal anti-calbindin-d28k antibody was raised in rabbit against calbindin-d28k purified from bovine cerebellum and shows no cross-reactivity with other brain peptides, including calretinin, vasoactive intestinal polypeptide, somatostatin, substance P, and neuropeptide Y (Buchan and Baimbridge, 1988; Meek et al., 2008). Western blot analysis of the antibody detected a single band of 28 kD (Buchan and Baimbridge, 1988; Bell et al., 2005; Meek et al., 2008). According to the manufacturer and the scientific literature (Buchan and Baimbridge, 1988; Conde et al., 1994; Zahm et al., 1996; Bouilleret et al., 2000), specific immunostaining with the antibody was completely abolished by preadsorption with calbindin-d28k, which according to Buchan and Baimbridge (1988) was at a final concentration of 1 nM.

The polyclonal anti-neurotensin antibody was raised in rabbit against synthetic peptide (human) neurotensin coupled to bovine thyroglobulin with glutaraldehyde and shows no cross-reactivity with other brain peptides, including neurokinin A, neurokinin B, somatostatin, and neuropeptide K (ImmunoStar; cf. Geisler and Zahm, 2006b). According to the manufacturer and the scientific literature (Zahm et al., 1996, 2011; Geisler and Zahm, 2006b), specific immunostaining with the antibody was completely abolished by preadsorption with a final concentration of 10 μg/ml neurotensin. No staining was observed when any of the three primary antibodies was omitted, which controlled for the secondary antiserum.

Designation of single units to subregions of the VP

Designation of single units to subregions of the VP was made by a scorer blind to changes in FR during self-administration. If all implanted microwire tracks were identified from their entry into cortex to their tips (blue spots marked by potassium ferrocyanide staining of iron deposits), microwire tip positions were subsequently histologically localized. If any of the implanted microwires could not be identified, neural data from the animal were discarded. To be designated into the VPvm, single units belonging to potassium ferrocyanide-stained tissue from microwire tips were localized 1) within substance P immunoreactivity and 2) within neurotensin immunoreactivity and 3) were absent from calbindin-d28k immunoreactivity (Zahm and Heimer, 1988, 1990; Zahm, 1989; Zahm et al., 1996). To be designated into the VPdl, single units belonging to potassium ferrocyanide-stained tissue from microwire tips were localized 1) within substance P immunoreactivity and 2) within calbindin-d28k immunoreactivity 3) and were absent from neurotensin immunoreactivity (Zahm et al., 1996; Riedel et al., 2002; Tripathi et al., 2010).

Training analysis

Outcome variables, e.g., criterion head movements, self-administered mg/kg/day, were analyzed as a function of 14 training days using repeated-measures ANOVAs (PASW 18.0.0; SPSS, Chicago, IL). When the assumption of sphericity was not confirmed, a Greenhouse-Geisser correction was used, which adjusts the degrees of freedom in the ANOVA to be more conservative. Fourteen training days was selected because this

was the time of the earliest recording session. Alpha criterion for all tests was 0.05.

Video analysis

A video frame-counter (VC-436; Thalner Electronics, Ann Arbor, MI) connected to the neuronal clock (CTR05; Measurement Computing, Norton, MA) time stamped each frame in a videocassette recorder (JVC HR-DD84OU; JVC, Wayne, NJ), which was used to monitor and record additional behaviors (approach and retreat, Fig, 1A,C, respectively) for off-line analysis (33 msec resolution).

Approach onset was determined by the start of a change in direction exhibited by the animal toward the photocell corner and culminated with the breaking of a photocell. Approach onset was typically a leftward or rightward head turn or a vertical head movement prior to head turning, consistent with the approach behaviors described by Chang and colleagues (1994, 1997, 2000). In the minority of cases for which animals initially faced the direction of the photocell corner while engaged in focused stereotypy, approach onset was determined as the start of alternating limb movements toward the photocell corner and culminated with the breaking of a photocell. Approach offset was determined by the first photocell break following the approach onset. Approaches and retreats in which the approach onset was less than 150 msec from a previous retreat offset (described below) were removed from analysis because of ambiguity in defining the offset of retreat and onset of approach. Approaches greater than 3 seconds in duration were excluded from analysis. Cued approaches were defined as approaches in which the S^D was on at approach onset, whereas uncued approaches were defined as approaches in which the S^D was off at approach onset. Cued responses were defined as criterion movements in which the S^D was on at response onset, and uncued responses were defined as criterion movements that occurred when the S^D was off. For cue analysis, an S^D trial that did not culminate in a self-administered cocaine infusion was defined as a miss and an S^D trial that culminated in a self-administered cocaine infusion was defined as a hit.

Retreat onset was determined by the start of a change in direction exhibited by the animal away from the photocell corner. In the vast majority of cases this was a leftward or rightward head turn, but in a minority of cases was a backward movement. The retreat offset was determined by the start of an additional change in direction exhibited by the animal or the start of a pause in locomotion of at least 66 msec (two video frames). For cases in which the animal's movement following retreat onset contained slight head bobbing or circular head movements during a continuous movement away from the photocell, these slight head movements were ignored and retreat offset was determined by the start of an overt additional change in direction exhibited by the animal. Retreats greater than 5 seconds in duration were excluded from analysis. Pump retreats were defined as retreats for which the pump was activated or deactivated within 2 seconds prior to or during a retreat, whereas nonpump retreats were all other retreats. Four example approach, response, and retreat events are displayed in Supporting Information Movie 1.

Neuronal analysis

Changes in FR were examined with respect to four events: cue, approach, response, and retreat. For each occurrence of an event, FR was calculated as number of spikes divided by the duration (seconds) of that particular event. Then, all of its occurrences within a session were grouped, and an average FR was determined. For the cue event, the objective was to minimize any contribution of movement to the assessment of FR. The average FR was calculated between S^D onset to $S^D + 150$ msec. For the approach event, the average FR was calculated between approach onset and approach offset (detailed in the Video analysis section). For the response event, the average FR was calculated between criterion movement onset and criterion head movement offset (detailed in the Head movement task section). For the retreat event, the average FR was calculated between retreat onset and retreat offset (detailed in the Video analysis section). Changes in FR were visualized in Matlab (The Mathworks, Cambridge, MA) with raster and perievent time histograms (PETHs), the code of which was modified from Ma (2010).

Firing rates during the time points described above were considered potential "signals" during behavior. These signals were compared with a baseline period for standardized "signal:baseline" ratios using a $B/(A + B)$ formula, termed the *directional change in FR*, where B is the signal and A is the baseline. For the cue event, the baseline was the average FR during the 150 msec prior to cue onset, as previously used (Ghitza et al., 2003). Precue FR was not likely related to any particular movement because behavior was "randomized" in that cues were presented noncontingently. Similarly, cue-evoked movements were prevented from influencing postcue FR assessments because their onset latency after S^D onset was >150 msec (Ghitza et al., 2003). For approach, response, and retreat events, the baseline was the average FR during the period from -6 to -3 seconds prior to criterion movements, as previously used (Ghitza et al., 2004, 2006). If within the baseline periods any photocell beam break, approach onset or offset, retreat onset or offset, or pump onset or offset occurred, that particular trial was omitted from calculating the

baseline. The directional change in FR ranged between 0 and 1, with a value of 0.5 indicating no change from baseline, values less than 0.5 a decrease in FR from baseline, and values greater than 0.5 an increase in FR from baseline. Because VP neurons exhibit changes in FR surrounding cocaine-reinforced responses with heterogeneous decreases or increases in FR (Root et al., 2010), a second analysis was conducted on all events termed the *absolute change in FR*. The absolute change in FR was calculated using the formula $|directional\ change\ in\ FR - 0.5|$. The absolute change in FR ranged between 0 and 0.5 (where 0 = no change from baseline FR) and represents change in FR from baseline regardless of whether the change was a decrease or increase in FR (Ghitza et al. 2006). For all analyses (cues, responses, approaches, and retreats), events that occurred during the initial 10 rapidly spaced "loading" self-infusions were excluded in order to minimize the influence of pharmacological differences between events.

To evaluate subregional differences in the magnitude of changes in FR between VPvm and VPdl neurons, Mann-Whitney U tests evaluated the absolute change in FR for cue, approach, response, and retreat events, as previously used (Ghitza et al., 2004, 2006; Fabbricatore et al., 2010). Mann-Whitney U tests were necessary because these data did not fit a normal distribution. If a significant difference was observed between subregions using the absolute change in FR during approach, response, or retreat, we examined whether the populations exhibited differential increases/decreases in FR by using the Mann-Whitney U test on the directional changes in FR for that specific behavior. To examine differences in FR during cued and uncued behaviors, correlation coefficients from each subregion were computed using the directional change in FRs (e.g., the correlation coefficient of cued approach directional change in FR and uncued approach directional change in FR). To analyze differential relationships between subregions, correlation coefficients of directional changes in FR values were compared by using a z-test as described by Morse (1999). To analyze subregional differences in the prevalence of recorded neurons in left vs. right hemisphere, biphasic vs. triphasic waveform profiles, and propensity to record from multisingle-unit microwires (single microwires that recorded more than one single unit), Fisher's exact test was used. All statistics were used at the population level rather than the single-neuron level, in order to not violate the statistical assumption of independence.

RESULTS

Behavior

Prior to recordings, all rats exhibited both task and skill learning. With regard to task learning, reaction time in response to the S^D decreased over days, $F(4.040,96.970) = 99.468$, $P < 10^{-32}$ (Greenhouse-Geisser corrected; Fig. 2A). Over training sessions, probability of self-infusion upon S^D presentation, $F(4.424,106.173) = 24.792$, $P < 10^{-14}$ (Greenhouse-Geisser corrected; Fig. 2B), and total drug intake (mg/kg), $F(4.980,119.530) = 8.647$, $P < 10^{-6}$ (Greenhouse-Geisser corrected; Fig. 2C), increased. Animals escalated their intake of cocaine over days, decreasing the latency to reach the tenth self-infusion, $F(3.886,85.487) = 5.133$, $P < 0.001$ (Greenhouse-Geisser corrected; Fig. 2D).

With regard to skill learning, the number of criterion movements increased over days, $F(4.948,118.759) = 33.18$, $P < 10^{-20}$ (Greenhouse-Geisser corrected; Fig. 2E), whereas the number of inverse criterion movements (downward movements starting at or above photocell 5 and ending at photocell 2 or below, and without programmed consequence) did not change, $F(1.907,45.762) = 2.116$, $P > 0.05$ (Greenhouse-Geisser corrected). Over the last 3 days of training, the latency for the subsequent movement following a criterion movement was 19.26 ± 2.77, 17.80 ± 2.97, and 16.76 ± 2.75 seconds, demonstrating that criterion movements were inconsistent with stereotypic head bobbing. The average velocity of criterion movements increased over days, $F(3.532,84.775) = 9.480$, $P < 10^{-5}$ (Greenhouse-Geisser corrected; Fig. 3A), as a function of decreased duration, $F(2.816,67.583) = 20.747$, $P < 10^{-8}$ (Greenhouse-Geisser corrected; Fig. 3B) but not distance, $F(13,312) = 1.147$, $P > 0.05$ (Greenhouse-Geisser corrected; Fig. 3C). The probability of starting the criterion movement at the minimum requirement, photocell 2, increased over days, $F(6.193,154.828) = 2.533$, $P < 0.05$ (Greenhouse-Geisser corrected; Fig. 3D). The probability of ending a criterion movement at the minimum requirement, photocell 5, did not change, $F(4.686,112.469) = 1.045$, $P > 0.05$ (Greenhouse-Geisser corrected; Fig. 3E).

In summary, animals learned the self-administration task, which consisted of a vertical head movement operant. Animals escalated their intake of drug, posited to exemplify "addiction-like behavior" in rats (Ahmed and Koob, 1998; Deroche-Gamonet et al., 2004). Although it was not required, animals became skilled and efficient in their use of the vertical head movement operant, consistent with our previous examination (Root et al., 2011) and hypothesized to occur in highly experienced human drug users (Tiffany, 1990).

Histological localization and baseline single-unit properties

Neurons were recorded typically on day 16 of training (average), ranging between days 14 and 24. Among the

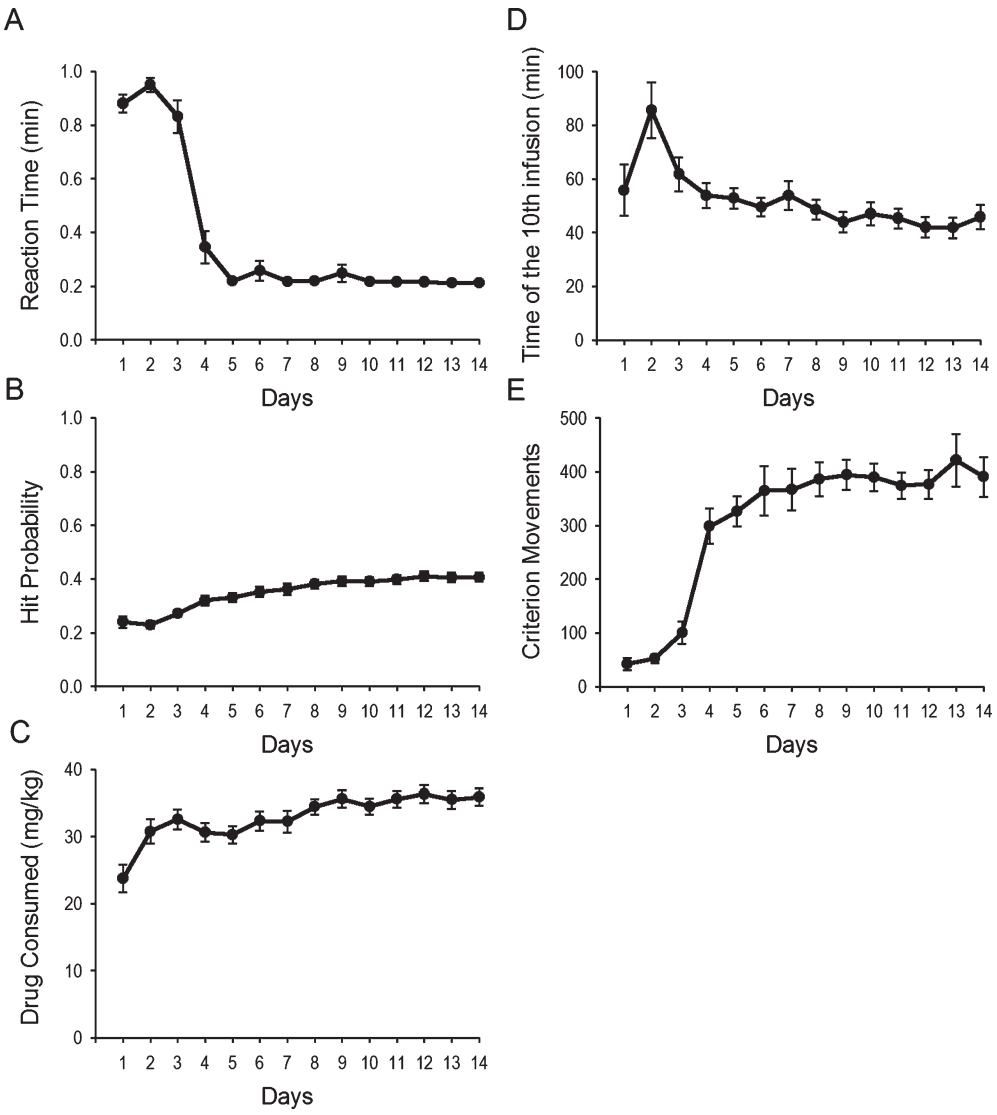

Figure 2. Self-administration and cue learning. Reaction time in response to the S^D (**A**), probability of self-administering cocaine upon S^D presentation (**B**), cocaine consumption (**C**), latency to load up to the tenth infusion (**D**), and number of criterion movements (**E**). Values are average ± SEM (*y* axes) per day (x axes).

400 microwires implanted within the basal forebrain of 25 rats, 202 microwires were localized to the VP. Among these, 38 microwires were localized to the VPdl (Fig. 4A–I displays three examples; Fig. 5 shows all microwires as blue triangles), recording 48 single units. In total 140 microwires were localized to the VPvm (Fig. 4J–R displays three examples; Fig. 5 shows all microwires as black circles), recording 171 single units. Twenty-four microwires recording 24 single units were removed because of histological localization to all three stains, which typically occurred at the most caudal, sublenticular aspects of VP. The amplitude and signal-to-noise ratio of VP neurons (Table 2) did not differ between subregions (all $|z| < 1.84$, $P > 0.05$). The prevalence of recording from multiple single-unit microwires, nine of 38 (23.6%) VPdl and 24 of 140 (17.14%) VPvm microwires, did not differ between subregions (Fisher's exact test, $P > 0.05$). The vast majority of single units exhibited an initial negativity in the waveform, consistent with our previous examination (Root et al. 2010). A minority of single units exhibited an initial positivity prior to the valley of the waveform (triphasic profile), four of 48 (8.33%) in VPdl and 20 of 171 (11.70%) in VPvm, the prevalence of which did not differ between subregions (Fisher's exact test, $P > 0.05$). The prevalence of single units recorded from microwires within the right vs. left hemisphere, with 20 of 48 (41.67%) VPdl and 88 of 171 (51.46%) VPvm single units recorded from the right hemisphere, did not differ between subregions (Fisher's exact test, $P > 0.05$). The cue baseline FRs (Table 2) and behavior baseline FRs (Table 2) did not differ between subregions (all $|z| < 0.28$, $P >$

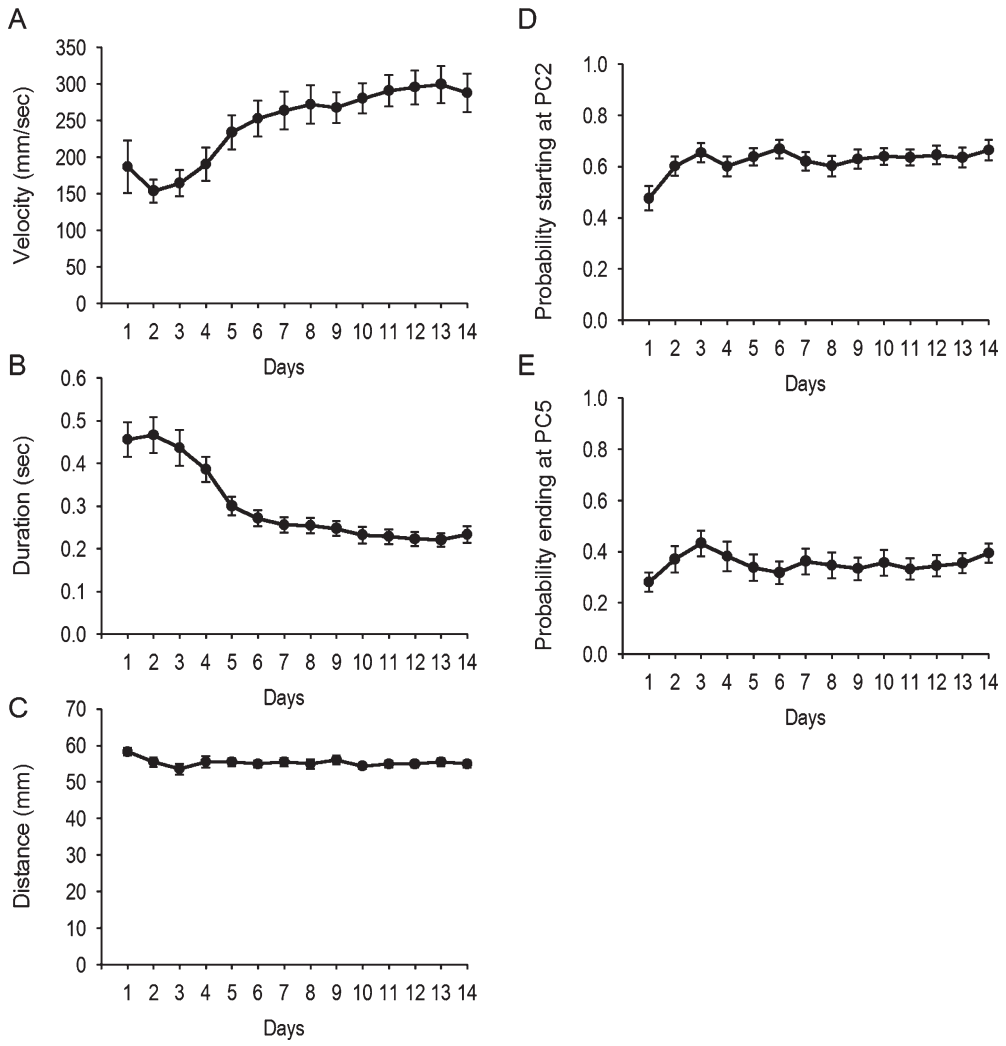

Figure 3. Skill learning: changes in criterion head movement parameters with extensive repetition. Changes in velocity (**A**), duration (**B**), distance (**C**), probability of starting at photocell 2, minimum required for a criterion movement (**D**), and probability of ending at photocell 5, minimum required for a criterion movement (**E**). Values for A–C are average median ± SEM per day for criterion head movements (y axes). Values for D,E are average probability ± SEM. All x axes refer to training day.

0.05). Overall, these results demonstrate that waveforms and baseline FRs of recorded neurons were not statistically different between VP subregions and hemispheres.

Analytical strategy

During cocaine self-administration, subsets of NAcc neurons exhibit changes in FR prior to response completion, following response completion, or in both time periods (Hollander and Carelli, 2005; Ghitza et al., 2004, 2006; Fabbricatore et al., 2010). In the present study, in which we have specifically isolated approach, response, and retreat behaviors, 85.42% of VPdl and 76.02% of VPvm neurons exhibited at least a 20% change in FR during one, or any combination of two or three, of these behaviors (see Table 4). See Table 3 for average ± SEM number of approach, response, and retreat events per animal and their average ± SEM durations (msec) used in electrophysiological analyses. VP neurons were distributed into smaller subsets of neurons across the different components of the task. Therefore, the following results are organized by neurons that exhibited changes in FR during one behavior only, two behaviors, and finally all three behaviors. Furthermore, we tested whether changes in FR during these behaviors, as well as the correlations of changes in FR between different behaviors, differed between VPdl and VPvm subregions. The major differences between VP subregions occurred during approach and response components of self-administration. First, VPdl neurons exhibited a larger change in FR than VPvm neurons during approach or response. In addition, changes in FR by VPdl neurons typically began during

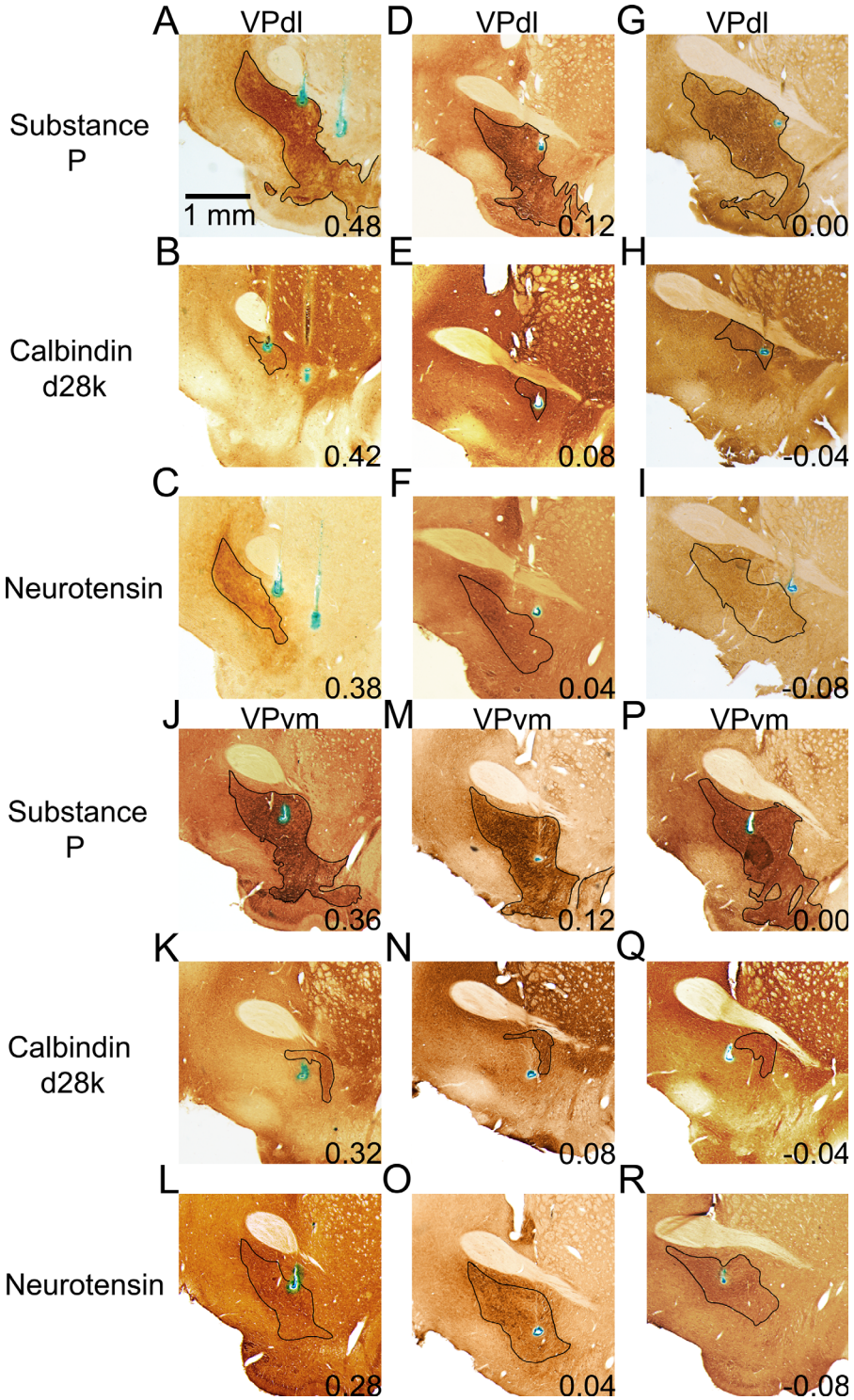

Figure 4. Example microwires localized to VP subregions. Examples are displayed in groups of three. A–I display three examples of microwires localized to the VPdl in three vertical panels each; example 1 (**A–C**), example 2 (**D–F**), and example 3 (**G–I**). J–R display three examples of microwires localized to the VPvm in three vertical panels each; example 1 (**J–L**), example 2 (**M–O**), and example 3 (**P–R**). A,D,G,J,M,P display substance P immunohistochemistry. B,E,H,K,N,Q display calbindin-d28k immunohistochemistry. C,F,I,L,O,R display neurotensin immunohistochemistry. Green/blue dot in each panel is an iron deposit from the uninsulated microwire tip visualized from by potassium ferrocyanide counterstain. Numbers refer to approximate anteroposterior coordinate based on Paxinos and Watson (2005). As a model for all VPdl neurons recorded, VPdl example 1 (A–C) displays two microwire tip locations. The wire closest to the anterior commissure was localized to substance P immunoreactivity (A) and calbindin-d28k immunoreactivity (B) but not neurotensin immunoreactivity (C). The microwire farthest from the anterior commissure (A) was localized outside of substance P immunoreactivity and therefore excluded from the data set. As a model for all VPvm neurons recorded, VPvm example 1 (J–L) displays a microwire tip location localized to substance P immunoreactivity (J) and neurotensin immunoreactivity (K) but not calbindin-d28k immunoreactivity (L). Any tissue from the right hemisphere has been rotated horizontally to the left hemisphere for the sake of uniform orientation (midline is left for all panels). Outlines were based on substance P, calbindin-d28k, and neurotensin immunoreactivity; the atlas of Paxinos and Watson (2005); and the scientific literature (Zahm and Heimer, 1988, 1990; Zahm 1989; Zahm et al., 1996; Riedel et al., 2002; Tripathi et al., 2010). All sections were 40 μm thick. Scale bar = 1 mm.

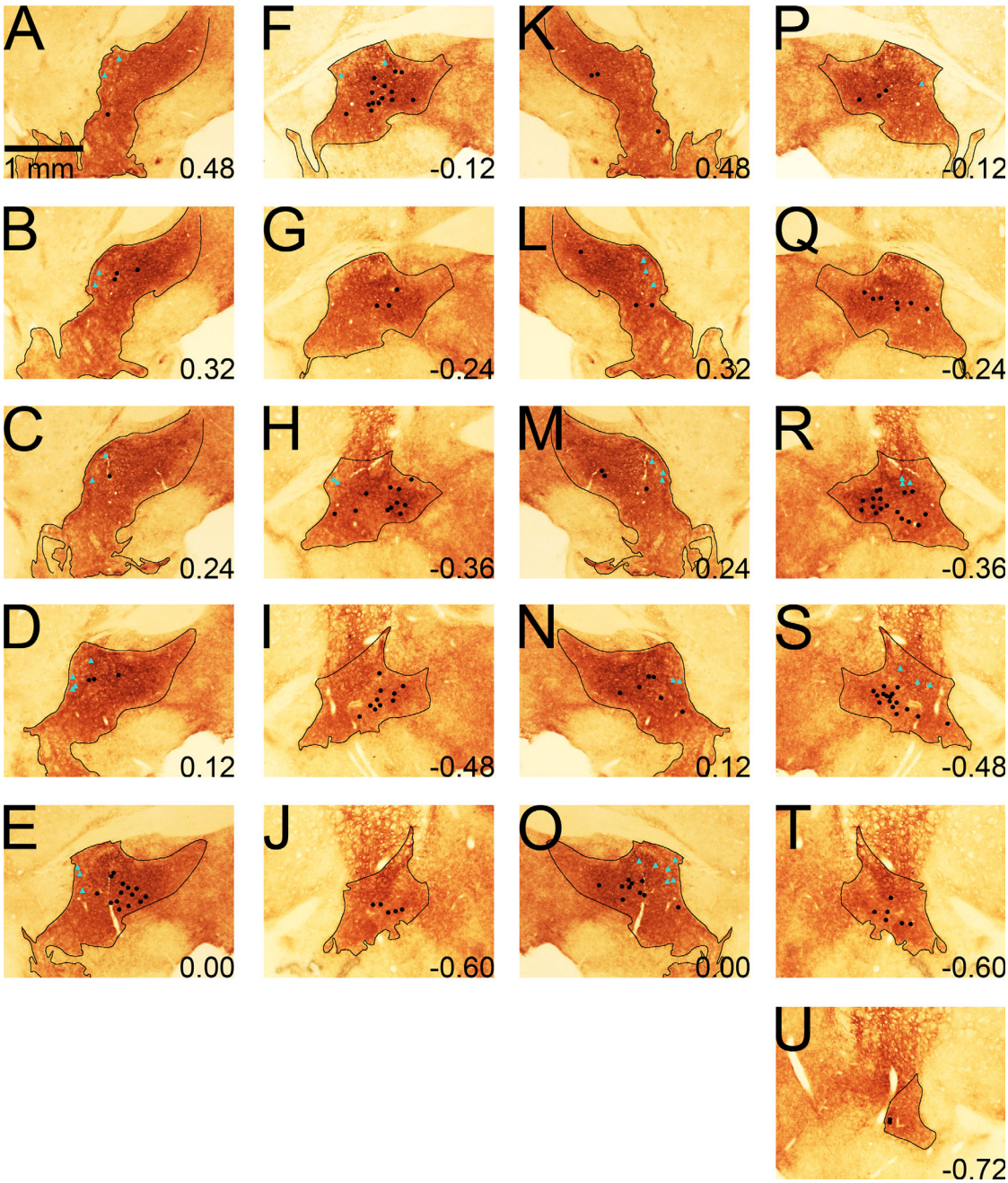

Figure 5. All microwires from all rats that were localized to VP subregions. Tissue displayed is substance P immunoreactivity from the left hemisphere of a rat used in the present data set. The left hemisphere implant from this rat was misplaced dorsal to VP and thus unencumbered by microwire tip counterstaining and therefore was selected for display purposes. Black circles and cyan triangles indicate VPvm and VPdl localized microwires, respectively. **A–J** display right hemisphere-localized microwires (midline right). **K–U** display left hemisphere-localized microwires (midline left). Outlines were based on substance P immunoreactivity as well as the atlas of Paxinos and Watson (2005). Numbers refer to approximate anteroposterior coordinate based on Paxinos and Watson (2005). All sections were 40 μm thick. Scale bar = 1 mm.

the approach and carried through the response in the same direction with similar or greater magnitude. In contrast, VPvm neurons exhibited significantly weaker changes in FR during approach and response, as well as a significantly weaker relationship of changes in FR between approach and response.

Changes in FR during one of three self-administration behaviors

The three behaviors investigated here (approach, response, and retreat), are important for different reasons. The approach can be considered a cocaine-seeking behavior, whereas the response can be considered a

TABLE 2.
Electrophysiological Data by Subregion[1]

Subregion	Units (n)	Triphasic (%)	Amplitude (μV)[2]	Signal-to-noise ratio	Baseline FR (cue)	Baseline FR (behaviors)
VPdl	48	8.33	116.55 ± 7.10	4.49 ± 0.20	0.95 ± 0.2	1.00 ± 0.22
VPvm	171	11.63	139.14 ± 6.33	4.22 ± 0.09	1.49 ± 0.35	1.52 ± 0.36
Total	219					

[1]Units and Triphasic refer to total number and percentage, respectively. All other data are presented as means ± SEM. VPvm, ventromedial ventral pallidum; VPdl, dorsolateral ventral pallidum.
[2]Amplitude of unitary action potentials.

TABLE 3.
Behavioral Events Used for Electrophysiological Analyses[1]

Behavior	No. of events per animal	Duration (msec)
Approach	608.96 ± 72.77	956.60 ± 63.08
Cued approach	310.60 ± 35.17	955.97 ± 63.83
Uncued approach	298.36 ± 38.98	960.40 ± 62.55
Criterion movement (response)	312.96 ± 41.72	340.20 ± 19.00
Cued response	147.52 ± 18.82	341.08 ± 18.88
Uncued response	165.44 ± 24.44	335.95 ± 20.52
Retreat	630.00 ± 75.09	694.92 ± 39.00

[1]Data are presented as mean ± SEM number of events per animal as well as mean ± SEM duration (msec).

cocaine-taking behavior. In contrast, the retreat is a behavior that might reflect the anticipated reward (cocaine infusion) for the immediately preceding completion of approach-response behaviors and/or a behavior that leads to the location of focused stereotypy. Woodward and colleagues (Chang et al., 1994, 1997, 2000) have shown that NAcc neurons exhibit changes in FR during distinct behaviors related to cocaine self-administration. We first investigated whether VP neurons discriminated the components of cocaine self-administration (approach, response, or retreat) and whether changes in FR during these behaviors differed between VP subregions. First, discrimination of different behaviors by VP neurons would demonstrate that the behaviorally coincident firing patterns observed in NAcc neurons during cocaine self-administration (Chang et al., 1994, 1997, 2000) are also observed in VP. Second, differential changes in FR between VP subregions during individual components of cocaine self-administration would elucidate the individual contributions of the ventral striatopallidal subcircuits.

Subpopulations of neurons that exhibited changes in FR during only the approach toward the photocell corner were observed in both VP subregions (Table 4). However, as a population during the approach, neurons of the VPdl exhibited a significantly larger absolute change in FR than neurons of the VPvm ($z = -3.30$, $P < 0.001$; Fig. 6A). Two examples of approach-related firing patterns are shown in Figure 6B (VPdl neuron) and Figure 6C (VPvm neuron). In each case, changes in FR occur at the onset of approach (Fig. 6B left, C left) and exhibit no change in FR during response (Fig. 6B center, C center) or retreat (Fig. 6B right, C right). Subregional differences were not observed for the approach when examining directional changes in FR, $z = -0.85$, $P > 0.05$, suggesting that approach-related firing was heterogeneous in direction for both subregions.

To examine the influence of the S^D upon approach-related firing patterns, approaches were sorted into cued and uncued trials. Between subregions, the VPdl exhibited larger cued (Fig. 6D) and uncued approach (Fig. 6E) absolute changes in FR than the VPvm (cued $z = -2.90$, $P < 0.01$; uncued $z = -2.26$, $P < 0.05$). Within the VPdl alone, a significant correlation was observed between cued and uncued approach directional changes in FR, VPdl $r = 0.69$, $P < 10^{-7}$ (Fig. 6F). Within the VPvm alone, cued and uncued approach directional changes in FR were also significantly correlated, VPvm $r = 0.73$, $P < 10^{-28}$ (Fig. 6G). The correlation coefficients did not differ between subregions, $z = -0.45$, $P > 0.05$. In other words, within each subregion, most neurons did not discriminate changes in FR between cued approach and uncued approach conditions. Two examples of similar firing patterns between cued and uncued approaches are displayed in Figure 6H for a VPdl neuron and in Figure 6I for a VPvm neuron. On the rare occasion when a difference existed between cued and uncued approach conditions, such neurons were located in the VPvm. Thus, it appears that the S^D during cocaine self-administration has little or no influence on approach-related firing patterns of individual neurons from either VP subregion.

The most common changes in FR of VP neurons occurred during only the response (criterion movement; Table 4). As a population during the response, neurons of the VPdl exhibited a significantly larger absolute change in FR than neurons of the VPvm ($z = -2.78$, $P < 0.01$; Fig. 7A). Two examples of response-related firing patterns are shown in Figure 7B (VPdl neuron) and Figure 7C (VPvm neuron). In both cases, FRs were altered during

TABLE 4.

Distribution of Neurons Within VP Subregions Exhibiting 20% Change in Firing Rate From Baseline (Increase, Decrease, or Mixed) During Distinct Behaviors[1]

	Increase (%/N)	Decrease (%/N)	Mixed (%/N)	Total (%/N)
Approach VPdl	4.17/2	6.25/3	NA	10.42/5
Approach VPvm	2.92/5	5.26/9	NA	8.19/14
Response VPdl	6.25/3	18.75/9	NA	25/12
Response VPvm	10.53/18	12.28/21	NA	22.81/39
Retreat VPdl	0/0	2.08/1	NA	2.08/1
Retreat VPvm	5.85/10	2.92/5	NA	8.77/15
Approach-response VPdl	2.08/1	10.42/5	2.08/1	14.58/7
Approach-response VPvm	1.75/3	5.85/10	1.75/3	9.36/16
Approach-retreat VPdl	4.17/2	2.08/1	0/0	6.25/3
Approach-retreat VPvm	2.34/4	2.34/4	1.17/2	5.85/10
Response-retreat VPdl	0/0	2.08/1	2.08/1	4.17/2
Response-retreat VPvm	1.75/3	2.34/4	7.02/12	11.11/19
Approach-response-retreat VPdl	6.25/3	12.5/6	4.17/2	22.92/11
Approach-response-retreat VPvm	2.92/5	3.51/6	3.51/6	9.94/17
Total VPdl	22.92/11	54.17/26	8.33/4	85.42/41
Total VPvm	28.07/48	34.5/59	13.45/23	76.02/130

[1]Data are presented as percentage and total number of neurons within a particular VP subregion (VPdl or VPvm). Total refers to number of neurons exhibiting 20% change from baseline. This categorization was intended for simplification purposes that were sensitive enough to detect relatively small changes in FR.

the response (Fig. 7B center, C center) but not the retreat (Fig. 7B right, C right). The VPvm neuron was not altered during the approach (Fig. 7C left), but the VPdl neuron (Fig. 7B left) exhibited an increase in FR just prior to the approach offset. Analysis of the directional changes in FR during the response revealed that the VPdl was significantly decreased in FR compared with the VPvm, $z = -2.18$, $P < 0.05$. The VPdl median directional change in FR during the response was 0.44 (approximately a 21% reduction in FR), and the VPvm median directional change in FR was 0.49 (less than 1% reduction in FR).

To examine the influence of the S^D on response-related firing patterns, responses were sorted into cued and uncued trials. Between subregions, the VPdl exhibited larger cued (Fig. 7D) and uncued (Fig. 7E) absolute changes in FR than the VPvm, cued $z = -2.68$, $P < 0.01$; uncued $z = -2.31$, $P < 0.05$. Within the VPdl alone, a significant correlation was observed between cued and uncued response directional changes in FR, VPdl $r = 0.38$, $P < 0.01$ (Fig. 7F). Within the VPvm alone, cued and uncued response directional changes in FR were also significantly correlated, VPvm $r = 0.56$, $P < 10^{-14}$ (Fig. 7G). The correlation coefficients did not differ between subregions, $z = -1.33$, $P > 0.05$. That is, within each subregion, neurons did not discriminate changes in FR between cued response and uncued response conditions (examples are displayed in Fig. 7H for a VPdl neuron and in Fig. 7I for a VPvm neuron). Outliers within Figure 7F,G suggested that a very small number of neurons discriminated between cued and uncued response conditions. However,

Figure 6. VPdl neurons exhibit greater changes in FR during the approach than VPvm neurons whether cued or uncued. **A:** Cumulative proportion of all neurons' absolute changes in FR during the approach per subregion. Gray and black lines indicate cumulative proportions for VPdl and VPvm neurons, respectively. Median values (0.50 proportion value) are displayed as circles (VPdl) and squares (VPvm). For this and all other cumulative proportion figures, the absolute changes in FR were used. A value of 0 was no difference from baseline FR, and a 50% change from baseline FR was 0.1. Examples of approach-related changes in FR are displayed from a VPdl neuron (**B**) and from a VPvm neuron (**C**). For B,C, rasters and PETHs are centered (time 0) around offset of approach (left), offset of response (center), and onset of retreat (right). Green dots in approach-raster and blue dots in response-raster indicate the onset of approach and onset of response, respectively. Red dots in retreat-raster indicate the offset of retreat. The cumulative proportions of all neurons' absolute changes in FR for cued approach and uncued approach per subregion are shown in **D** and **E**, respectively. Each VPdl (**F**) and VPvm neuron (**G**) directional change in FR during the cued approach (y axis) was plotted against its directional change in FR during the uncued approach (x axis). Each dot represents one neuron. Note that, for F,G, and all other scatterplot figures, directional changes in FR were used. In contrast to the absolute change in FR, a value of 0.5 was not different from baseline FR, and a 50% change from baseline FR was 0.6 (increase) or 0.4 (decrease). Two examples of similar directional changes in FR between cued and uncued approach changes in FR, one VPdl neuron (**H**) and one VPvm neuron (**I**), are displayed. For H,I, rasters and PETHs are centered (time 0) around offset of cued approach (left) and uncued approach (right). Green dots indicate the onset of approach. All rasters have been sorted for movement duration. Response rasters in B and C contain approximately half as many trials as approach and retreat rasters (Table 3); y axes of all PETHs refer to average FR (spikes/second) per trial. All raster and PETH x axes refer to time (msec). $*P < 0.05$ $**P < 0.01$, $***P < 0.001$.

visual inspection of these neurons' changes in FR determined that differences between cued and uncued response conditions were due to directional change comparisons (B/[A + B]), which exhibited low FRs under both A and B conditions (i.e., FR < 0.1 discharges/second that otherwise met all criteria for inclusion as individual units) that differed only slightly, rather than exhibiting clear patterned changes in FR during only cued or only uncued responses. Thus, similar to the approach, the S^D during cocaine self-administration has little or no

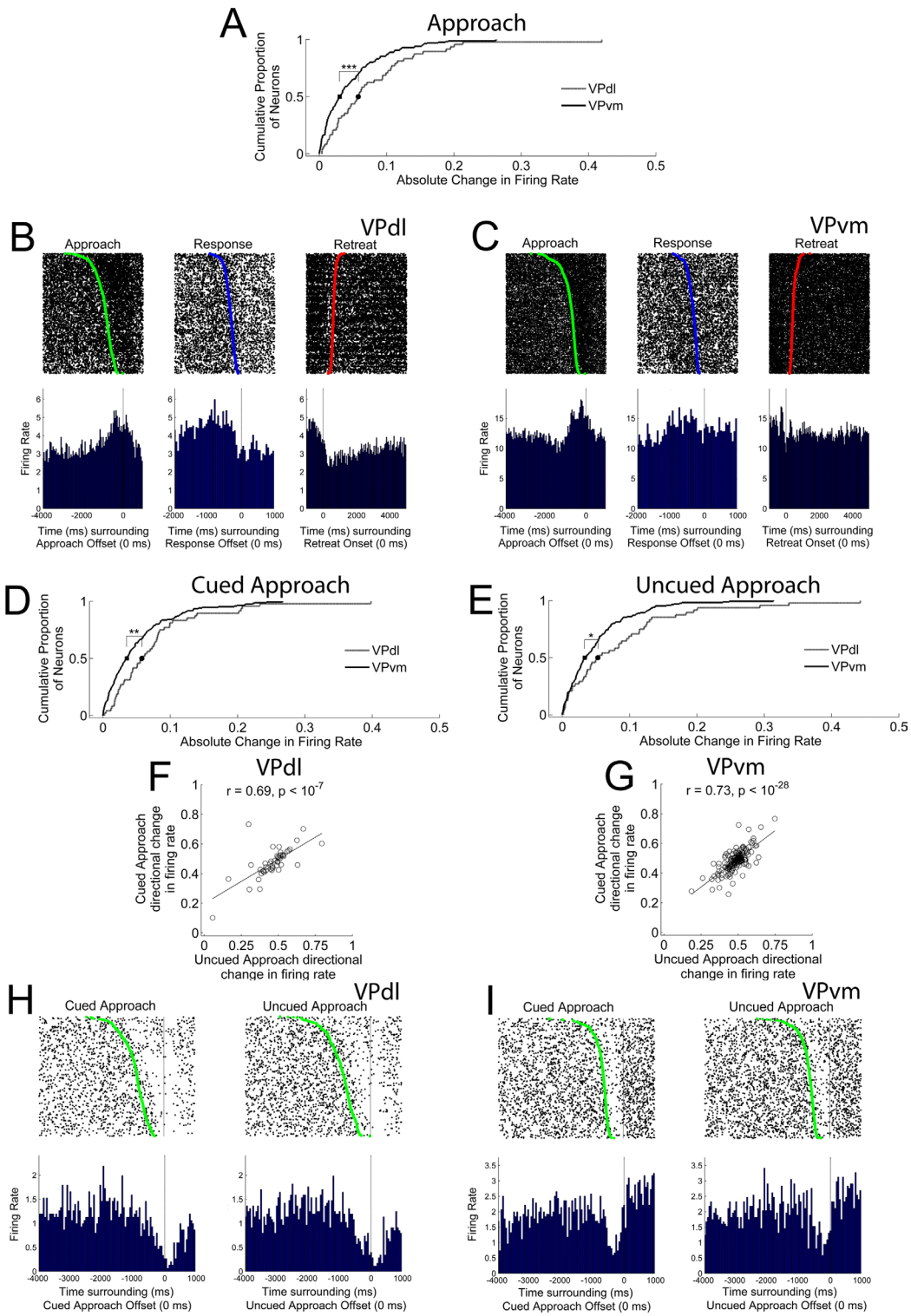

Figure 6 (legend on page 571).

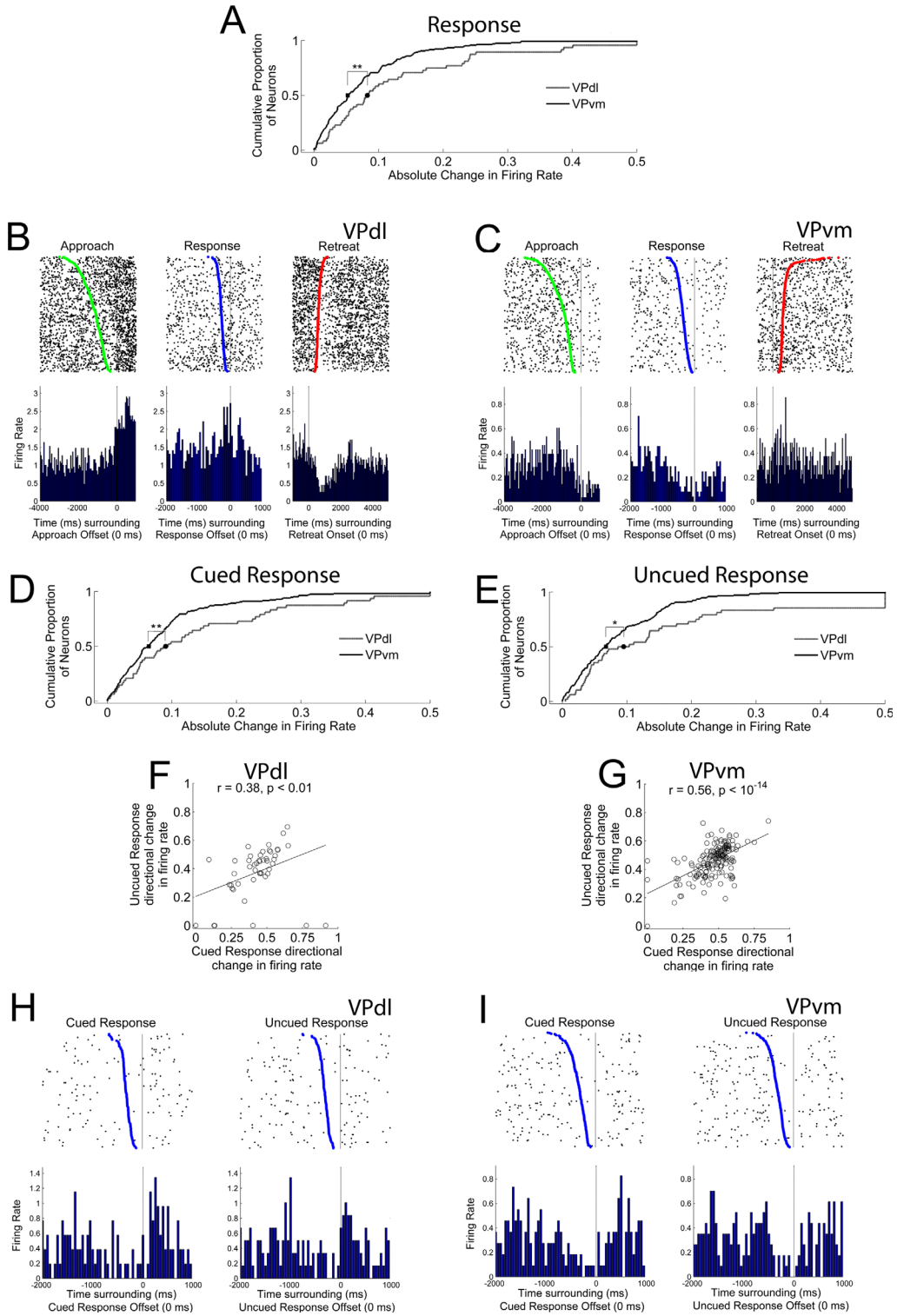

Figure 7. VPdl neurons exhibit greater changes in FR during the response than VPvm neurons whether cued or uncued. **A:** Cumulative proportion of all neurons' absolute changes in FR during the response per subregion. Gray and black lines indicate cumulative proportions for VPdl and VPvm neurons, respectively. Median values (0.50 proportion value) are displayed as circles (VPdl) and squares (VPvm). Examples of response-related changes in FR are displayed from a VPdl neuron (**B**) and from a VPvm neuron (**C**). For B,C, rasters and PETHs are centered (time 0) around offset of approach (left), offset of response (center), and onset of retreat (right). Green dots in approach-raster and blue dots in response-raster indicate the onset of approach and onset of response, respectively. Red dots in retreat-raster indicate the offset of retreat. The cumulative proportion of all neurons' absolute changes in FR for cued response and uncued response per subregion are shown in **D** and **E**, respectively. Each VPdl (**F**) and VPvm (**G**) neuron directional change in FR during the uncued response (y axis) was plotted against its directional change in FR during the cued response (x axis). Each dot represents one neuron. Two examples of similar directional changes in FR between cued and uncued response changes in FR, one VPdl neuron (**H**) and one VPvm neuron (**I**), are displayed. For H,I, rasters and PETHs are centered (time 0) around offset of cued response (left) and uncued response (right). Blue dots indicate the onset of response. All rasters have been sorted for movement duration. Response rasters in B and C contain approximately half as many trials as approach and retreat rasters (Table 3); y axes of all PETHs refer to average FR (spikes/second) per trial. All raster and PETH x axes refer to time (msec). $*P < 0.05$, $**P < 0.01$.

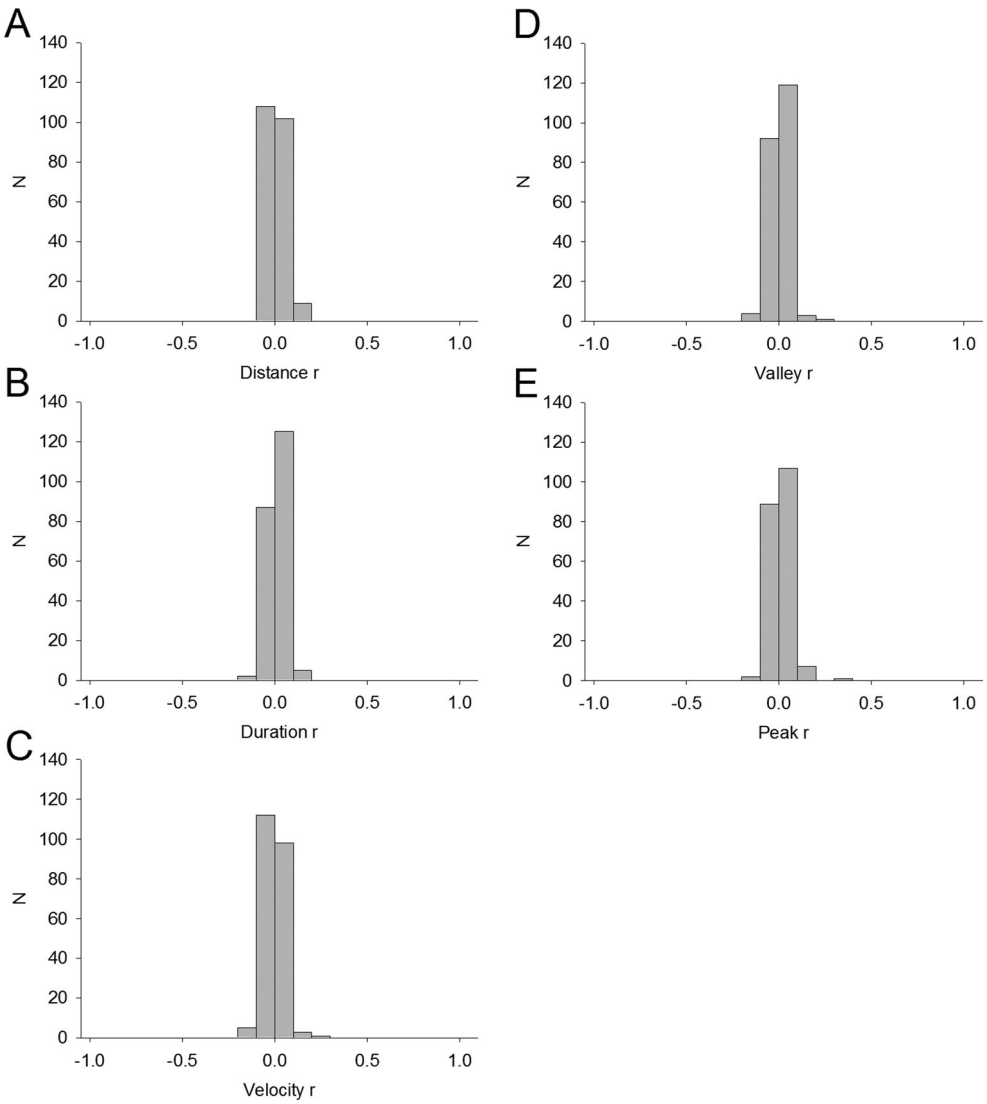

Figure 8. No relationship between response movement parameters and changes in FR by VP neurons. Given that no significant relationships were observed, all neurons were pooled into graphs of distance (**A**), duration (**B**), velocity (**C**), valley (start position; **D**), and peak (end position; **E**) regardless of subregion. Each bin on the x axis is 0.10. y Axis is frequency of occurrence (number of neurons exhibiting the r value).

influence on response-related firing patterns within neurons from either VP subregion.

No VP neurons exhibited any significant relationship of FR with vertical head movement properties, including distance (Fig. 8A), duration (Fig. 8B), velocity (Fig. 8C), start position/valley (Fig. 8D), or end position/peak (Fig. 8E). This is in contrast to head-movement neurons of the dorsolateral striatum, which exhibit exquisite sensitivity to these movement parameters with FR, as measured during similar motivated behavior (Pederson et al., 1997; Tang et al., 2007; Pawlak et al., 2010).

Fewer neurons exhibited their only change in FR during the retreat from the photocell corner (Table 4). No significant differences were found between subregions for the absolute changes in FRs during the retreat, $z = -0.92$, $P > 0.05$ (Fig. 9A). Among neurons that exhibited a retreat-only firing pattern, these neurons were typically located in the VPvm (Table 4; example neuron shown in Fig. 9B). In an attempt to identify the influence of cocaine infused prior to or during the retreat on changes in FR during retreat behavior, retreats were sorted into trials in which the pump was activated 2 seconds prior to the onset of retreat through the offset of the retreat vs. all other retreats, termed *pump retreats* and *nonpump retreats*, respectively.

Within VPdl alone, a significant correlation was observed between pump and nonpump retreat directional changes in FR, VPdl $r = 0.59$, $P < 10^{-4}$ (Fig. 9C). Within the VPvm alone, pump and nonpump retreat directional changes in FR were also significantly correlated, r =

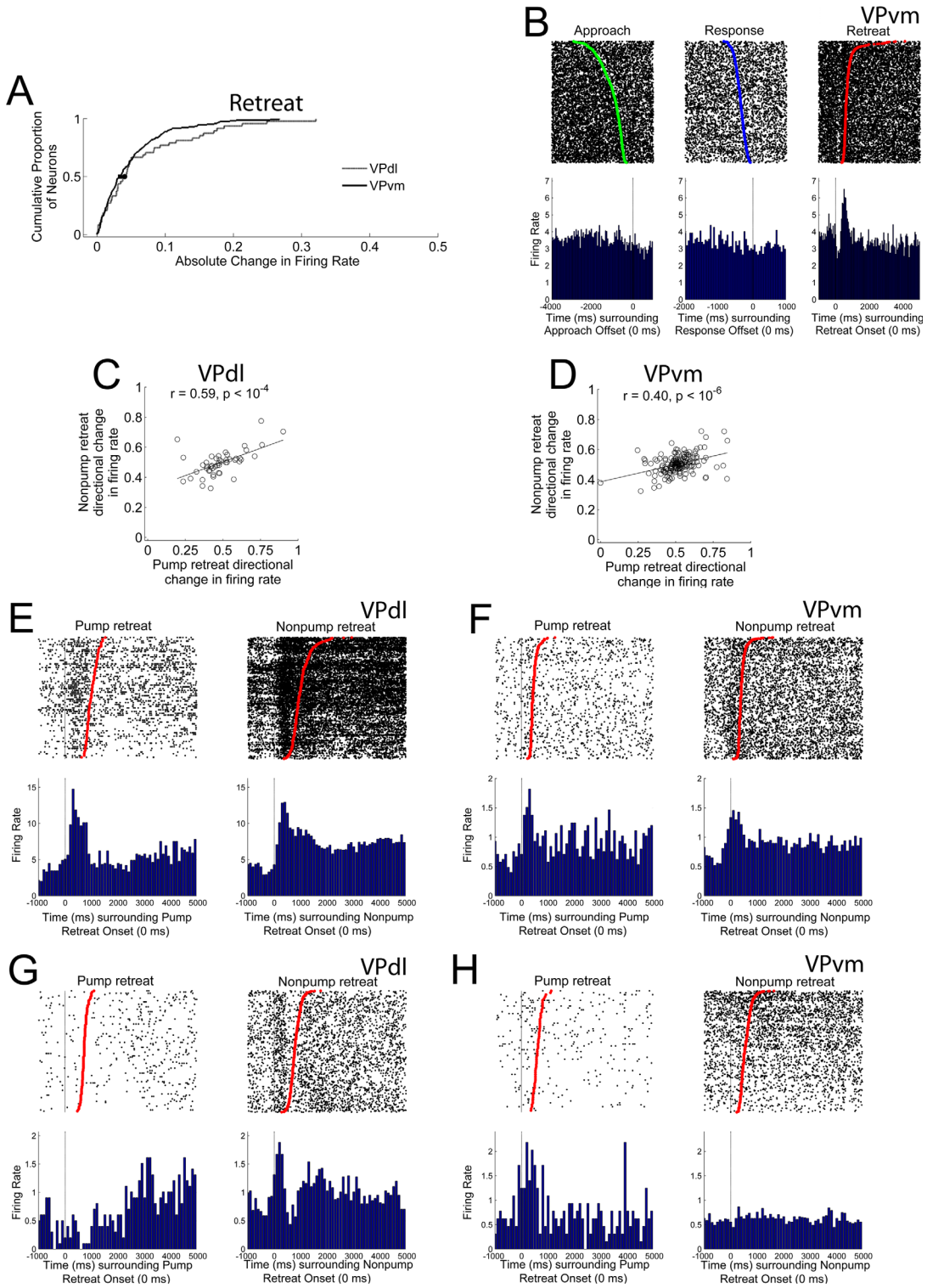

Figure 9. No differences between subregions during the retreat. Cumulative proportion of all neurons' absolute change in FR during the retreat per subregion. Gray and black lines in **A** indicate cumulative proportions for VPdl and VPvm neurons, respectively. Median values (0.50 proportion value) are displayed as circles (VPdl) and squares (VPvm) in A. One example of retreat-related firing is displayed in **B**, from a VPvm neuron. Raster and PETH are centered (time 0) around offset of approach (left), offset of response (center), and onset of retreat (right). Green dot in approach-raster and blue dot in response-raster indicate the onset of approach and response, respectively. Red dot indicates the offset of retreat. For each VPdl (C) and VPvm (D) neuron, the neuron's directional change in FR during the nonpump retreat (*y*-axis) was plotted against its directional change in FR during the pump retreat (*x*-axis). Each dot represents one neuron. Two examples of similar directional changes in FR between pump retreat and nonpump retreat changes in FR, one VPdl neuron (**E**) and one VPvm neuron (**F**), are displayed. Two examples of dissimilar directional changes in FR between pump retreat and nonpump retreat changes in FR, one VPdl neuron (**G**) and one VPvm neuron (**H**), are displayed. For E–H, rasters and PETHs are centered (time 0) around onset of pump retreats (left) and nonpump retreats (right). Red dots indicate the offset of the retreat. All rasters have been sorted for movement duration. Response raster in B contains approximately half as many trials as approach and retreat rasters (Table 3). Pump retreat rasters in E, F, G, and H contain approximately one quarter as many trials as nonpump retreat rasters; y axes of PETHs refer to average FR (spikes/second) per trial. Both x axes refer to time (msec).

0.40, $P < 10^{-6}$ (Fig. 9D). The correlation coefficients did not differ between subregions, $z = 1.65$, $P > 0.05$. That is, VP neurons' changes in FR largely did not discriminate between retreats with or retreats without pump activation. Two examples of similar changes in FR between pump and nonpump retreat conditions are shown for a VPdl neuron in Figure 9E and VPvm in Figure 9F. Nevertheless, some neurons exhibited differences in FRs between pump and nonpump retreat conditions in both subregions (VPdl neuron example in Fig. 9G and VPvm neuron example in Fig. 9H). It is possible that this minority of neurons plays a role in reward prediction, or it may be related to other factors not investigated here. In general, there appears to be little influence of the initial seconds of cocaine infusion prior to or during the retreat on changes in FR during retreat behavior.

In summary, 37.50% of VPdl and 39.77% of VPvm neurons exhibited at least a 20% change in FR during only the approach, only the response, or only the retreat (Table 4), suggesting that the behaviorally coincident firing patterns observed in NAcc neurons during cocaine self-administration (Chang et al., 1994, 1997, 2000) are projected to VP. VPdl neurons exhibited a significantly larger change in FR during approach or response than VPvm neurons, whether such approaches or responses were cued or uncued. Given that the NAcc core projects to the VPdl and NAcc shell projects to the VPvm, these results extend the repeated observation that core neurons exhibit greater changes in FR during cocaine-seeking behaviors than shell neurons (Ghitza et al., 2004; Hollander and Carelli, 2005; Fabbricatore et al., 2010). No differences between subregions were observed for changes in FR during the retreat. VP neurons did not discriminate between cued and uncued conditions for the approach or response and largely did not discriminate between retreats involving pump infusions or not. The S^D has little behavioral relevance during cocaine self-administration (Root et al., 2011), in contrast to S^D effects on abstinent drug-seeking (Ghitza et al., 2003; Root et al., 2009). The fact that VP changes in FR during approach and response during self-administration do not differ as a function of cue presentation suggests that VP neurons are engaged during conditions that are behaviorally relevant rather than those that are not relevant.

Changes in FR during two of three self-administration behaviors

We next examined whether VP neurons discriminated two of the three self-administration behaviors. Neurons that exhibit changes in FR during both approach and response might be related to processing the execution of drug-seeking and taking behaviors. Neurons that exhibit changes in FR during both approach and retreat, or during both response and retreat, might be involved in the association of cocaine-seeking behaviors with their expected reinforcement by cocaine.

When a change in FR occurred during the approach, VPdl neurons were highly likely to continue this change in FR in the same direction with similar or greater magnitude through the duration of the response (described briefly above for the VPdl neuron in Fig. 7B). Within the VPdl, a significant correlation was observed between the directional changes in FR during the approach and response, $r = 0.69$, $P < 10^{-7}$ (Fig. 10A). Two examples of VPdl neuron approach-response firing patterns are shown in Figure 10B,C. Although a significant correlation between the directional changes in FR during the approach and response was also observed within the VPvm, $r = 0.32$, $P < 10^{-4}$ (Fig. 10D), VPdl exhibited a significantly larger correlation coefficient than VPvm, $z = 3.11$, $P < 10^{-3}$. With the response directional change in FR as a dependent variable, this result was corroborated by an observed interaction between approach directional change in FR and subregion, $F(1,215) = 10.81$, $P < 0.01$. That is, the linear slopes of VPdl and VPvm neurons' relationship between approach and response differed between subregions. Taken together, although some VPvm neurons continued to change their FRs in the same direction from approach through response (example VPvm neuron in Fig. 10E), the weaker correlation of approach and response directional changes in FR by VPvm neurons suggests that this subregion exhibits more behavioral selectivity and thus more heterogeneous firing patterns, including approach-only or response-only changes in FR. In contrast, the stronger correlation of approach and response directional changes in FR by VPdl neurons suggests that this subregion might not typically discriminate drug-seeking from drug-taking during self-administration.

For neurons that exhibited a change in FR during the retreat, these were largely coupled with changes in FR during the approach, the response, or both the approach and response (Table 4). A significant correlation was observed for the directional changes in FRs during the approach and retreat within the VPdl alone, $r = 0.51$, $P < 0.001$ (Fig. 11A) and within the VPvm alone, $r = 0.41$, $P < 10^{-7}$ (Fig. 11B). Subpopulations of VP neurons exhibited a change in FR during approach, reverted back to baseline during the response, and exhibited another change in FR during the retreat (Fig. 11C,D, Table 4).

Other subpopulations of VP neurons exhibited changes in FR during response and retreat (Table 4). A significant correlation was observed for the directional changes in FRs during the response and retreat within the VPdl alone, $r = 0.37$, $P < 0.01$ (Fig. 11E) and within the VPvm alone, $r = 0.19$, $P < 0.05$ (Fig. 11F). Two examples of response-retreat

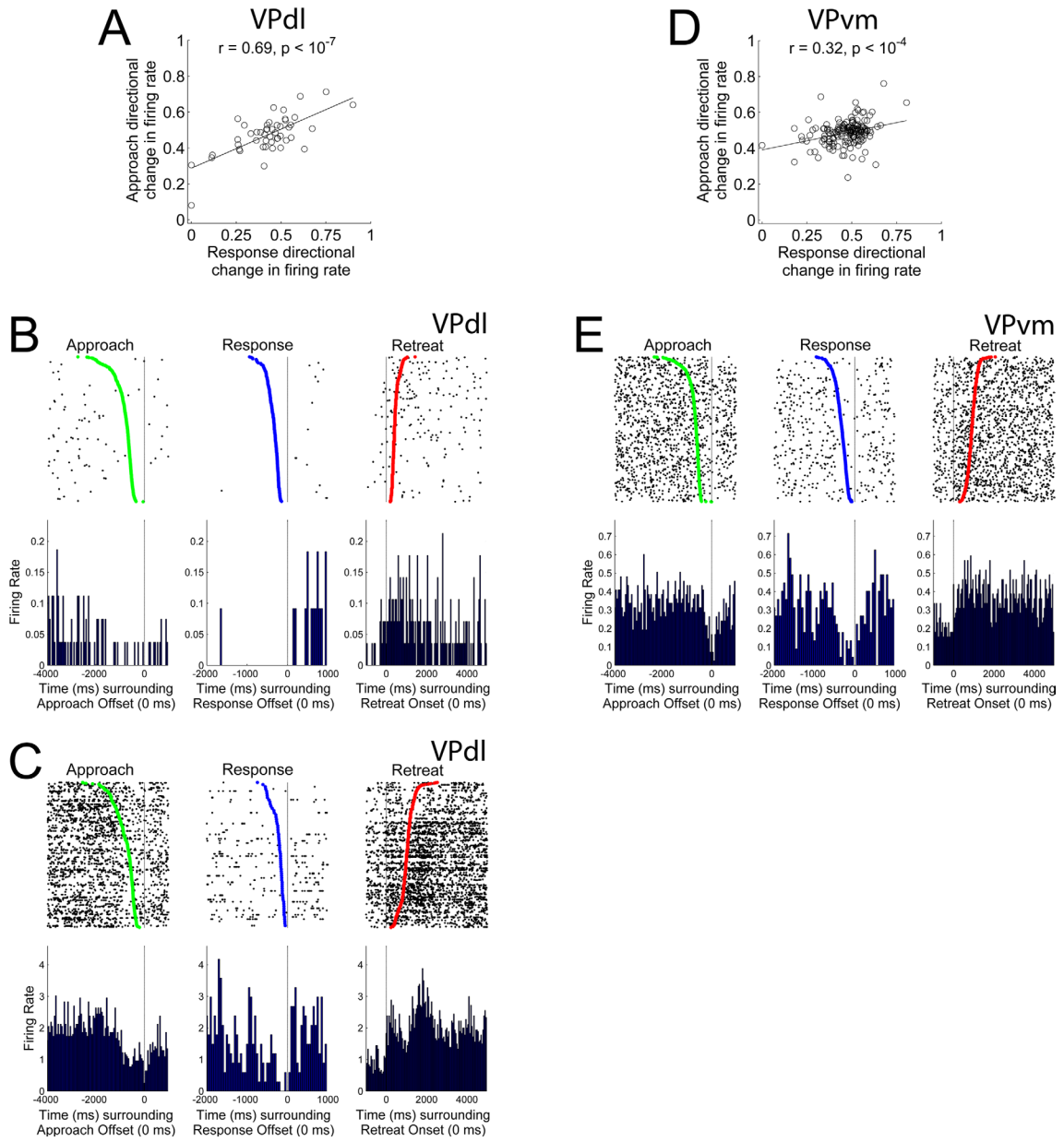

Figure 10. VPdl neurons exhibit a greater correlation between approach and response changes in FR than VPvm neurons. **A:** Each VPdl neuron's directional change in FR during the approach (y axis) plotted against its directional change in FR during the response (x axis). Each dot represents one neuron. Two example VPdl neurons exhibiting similar directional changes in FR from approach to response are displayed in **B,C**. **D:** Each VPvm neuron's directional change in FR during the approach (y axis) plotted against its directional change in FR during the response (x axis). Each dot represents one neuron. One example VPvm neuron exhibiting similar directional changes in FR from approach to response is displayed in **E**. Rasters and PETHs are centered (time 0) around offset of approach (left), offset of response (center), and onset of retreat (right). Green dots in approach-rasters and blue dots in response-rasters indicate the onset of approach and onset of response, respectively. Red dots in retreat-rasters indicate the offset of retreat. All rasters have been sorted for movement duration. Response rasters in B, C, and E contain approximately half as many trials as approach and retreat rasters (Table 3); y axis of PETH refers to average FR (spikes/second) per trial. Both x axes refer to time (msec).

firing patterns are displayed in Figure 11G for a VPdl neuron and in Figure 11H for a VPvm neuron. The correlation coefficients for approach-retreat and response-retreat did not differ between subregions (all $|z| < 0.74$, $P > 0.05$).

In summary, 25.00% of VPdl and 26.32% of VPvm neurons exhibited at least a 20% change in FR involving two behaviors, approach and response, approach and retreat, or response and retreat. VPdl neurons exhibited a significantly larger correlation coefficient between directional changes in FR between approach and response than VPvm neurons, suggesting that VPdl neurons uniquely participate in the execution of drug-seeking behaviors.

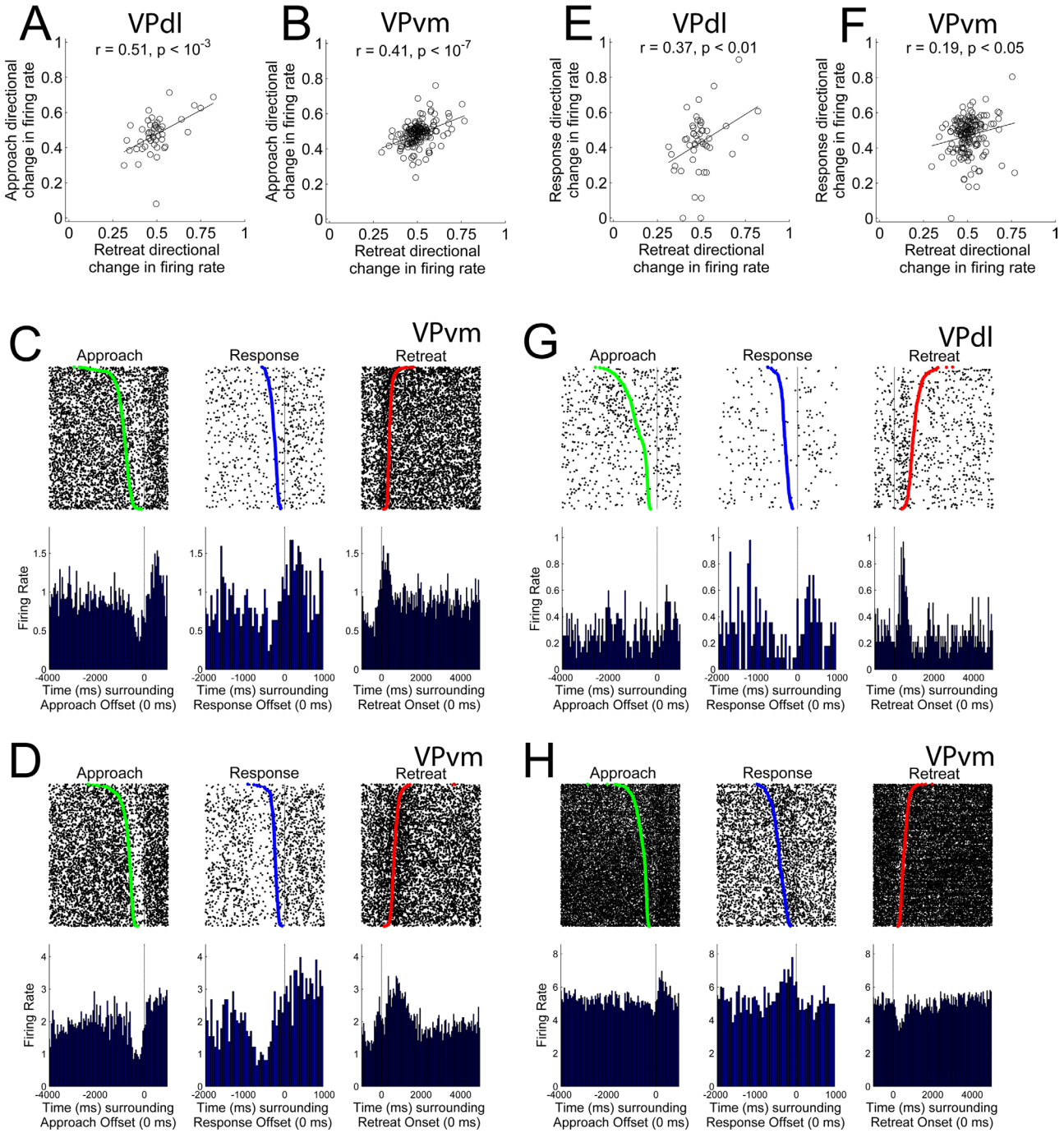

Figure 11. Correlations for other changes in FR during two behaviors, approach-retreat or response-retreat, did not differ between subregions. Each VPdl (**A**) and VPvm (**B**) neuron's directional change in FR during the approach (y axis) was plotted against its directional change in FR during the retreat (x axis). Each dot represents one neuron. Two examples of changes in FR during approach and retreat, but not during response, are displayed in **C,D**, both VPvm neurons. To examine response-retreat relationships, each VPdl (**E**) and VPvm (**F**) neuron's directional change in FR during the response (y axis) was plotted against its directional change in FR during the retreat (x axis). Each dot represents one neuron. Two examples of changes in FR during response and retreat, but not during approach, are displayed (**G** for VPdl neuron and **H** for VPvm neuron). For C,D,G,H, rasters and PETHs are centered (time 0) around offset of approach (left), offset of response (center), and onset of retreat (right). Green dots indicate onset of approach and blue dots indicate onset of response. Red dots indicate offset of retreat. All rasters have been sorted for movement duration. Response rasters in C, D, G, and H contain approximately half as many trials as approach and retreat rasters (Table 3); y axes of PETHs refer to average FR (spikes/second) per trial. Both x axes refer to time (msec).

The correlation coefficients of approach and retreat as well as response and retreat did not differ between subregions.

Changes in FR during all three self-administration behaviors

We next examined whether VP neurons exhibited changes in FR during all three behaviors. Such changes in FR might be considered a "gating" signal if they occur in the same direction (all increases or all decreases in FR), which has been observed in NAcc neurons (Taha and Fields, 2006). In contrast, such changes in FR might signal the contrasting components of different cocaine-seeking behaviors if they occur in heterogeneous directions.

Approximately 22.92% of VPdl and 9.94% of VPvm neurons exhibited at least a 20% change in FR during all three behaviors. Most of these neurons changed FR beginning at the onset of approach and continued in the same direction (increase or decrease in FR) through the response and retreat (Table 4; VPdl neuron example in Fig. 12A and VPvm neuron example in Fig. 12B), suggesting the possibility of a "gating" signal. A smaller population of neurons that exhibited a change in FR during approach, response, and retreat did so with heterogeneous directional changes in FR (Table 4, Fig. 12C,D shows VPdl neurons and Fig. 12E-H shows VPvm neurons).

Cue

Clear examples of changes in FR following S^D onset were not observed. With respect to absolute changes in FR in response to the cue, no significant differences were found between subregions, $z = -0.93$, $P > 0.05$ (data not shown). After sorting cue trials into those in which the animal self-administered cocaine (hits) vs. those in which the animal did not self-administer cocaine (misses), no differences between subregions were found for the absolute changes in FR (all $|z| < 1.16$, $P > 0.05$). Furthermore, no clear examples of changes in FR during hit or miss trials were observed. In summary, VP neurons were not sensitive to the onset of the S^D during cocaine self-administration, whether the trial was reinforced or not.

Examination of "initiation"-related firing patterns

The final analysis investigated whether VP neurons exhibited firing patterns prior to approach onset (i.e., pre-movement or initiation firing patterns). Such changes in FR have been observed in NAcc neurons (Chang et al., 1994) but were tacitly postulated to occur in VP neurons during the "initiation" of motivated behaviors (Mogenson et al., 1980). Visual inspection of all neurons' firing patterns revealed only three candidate neurons with changes in FR that began prior to the approach onset (Figs. 13A left, B left, C left). The two neurons displayed in Figure 13A,B were recorded from the same rat, and we returned to the recorded videos to reanalyze the self-administration behaviors. This rat exhibited a locomotor movement (alternating limb movements) toward a specific corner of the chamber just prior to the approach toward the photocell corner, which was termed the *pre-approach movement* (Supp. Info. Movie 2). Overlaying the pre-approach movement onset and offset (magenta and cyan dots in Figs. 13A right and 14B right, respectively) over the two candidate neuron rasters clearly demonstrated that the decrease (Fig. 13A second from right) or increase (Fig. 13B second from right) in FR prior to approach (time zero) was related to the pre-approach *movement*. The final candidate neuron, shown in Figure 13C, was recorded in a different rat and exhibited a decrease in FR prior to the approach onset (Fig. 13C left). For this neuron, we examined whether previous approaches (Fig. 13C third from right), responses (Fig. 13C second from right), or retreats (Fig. 13C right) explained the decrease in FR prior to the approach. Figure 13C (right) demonstrates that this rat often reapproached the operandum quickly following retreat offset and that a decrease in FR occurred in these trials near the offset of retreat. In summary, with respect to the behaviors studied in the present cocaine self-administration task, changes in FR of 219 VP neurons in no case preceded the onset of approach but rather occurred strictly *during* approach, response, and/or retreat behaviors.

DISCUSSION

A major goal in systems neuroscience and neurobiology of drug abuse is characterization of the unique contributions of specific brain subregions that underlie drug-seeking behavior. The present results extend neuroanatomical studies of VP subregional afferent and efferent projection patterns (Zahm and Heimer, 1988, 1990; Groenewegen et al., 1993; Bell et al., 1995; Kalivas et al., 1993; Zahm et al., 1996; Churchill et al., 1996; Heimer et al., 1991, 1997; O'Donnell et al., 1997; Tripathi et al., 2010) by demonstrating differential changes in FR within VPdl and VPvm subregions during distinct components of cocaine-seeking behavior. Neurons within the calbindin-d28k-immunoreactive VPdl exhibited a greater absolute change in FR during the approach and response relative to neurons in the neurotensin-immunoreactive VPvm. This was the case for cued and uncued approaches as well as cued and uncued responses. Because the NAcc core projects to the VPdl (Zahm and Heimer, 1990; Groenewegen et al., 1993; Zahm et al., 1996; O'Donnell et al., 1997; Tripathi et al., 2010) and core neurons exhibit a greater change in FR over medial NAcc shell neurons

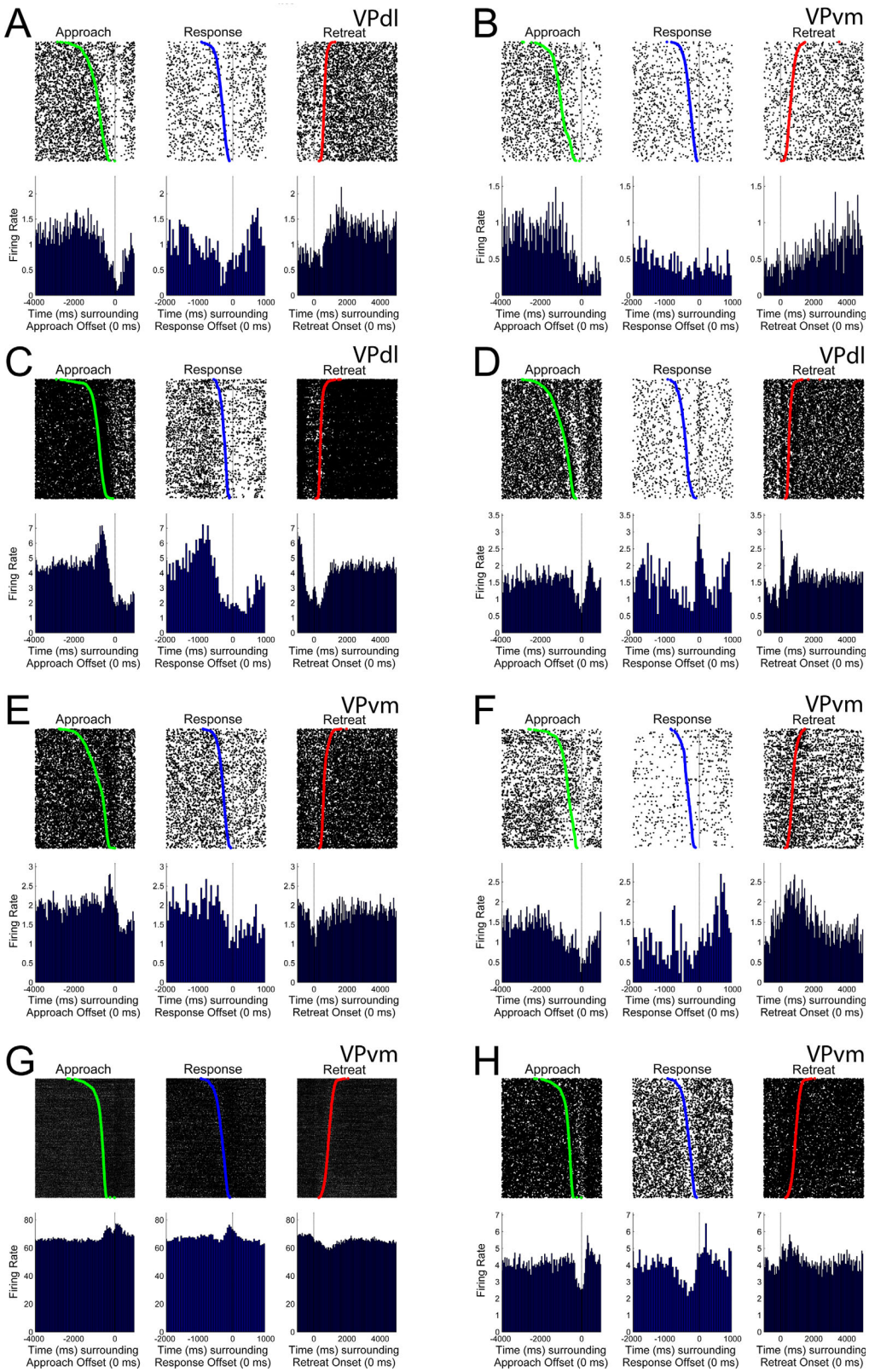

Figure 12. Changes in FR during all three behaviors, approach-response-retreat. Some neurons exhibited continuous directional changes in FR starting at the approach and continuing through the response and retreat. Two examples of similar directional changes in FR among approach, response, and retreat, one VPdl neuron (**A**) and one VPvm neuron (**B**), are displayed. Some neurons exhibited heterogeneous directional changes in FR among approach, response, and retreat changes in FR. Six examples of heterogeneous directional changes in FR among approach, response, and retreat changes in FR, two VPdl neurons (**C**,**D**) and four VPvm neurons (**E**–**H**), are displayed. For A–H, rasters and PETHs are centered (time 0) around offset of approach (left), offset of response (center), and onset of retreat (right). Green dots indicate onset of approach and blue dots indicate onset of response. Red dots indicate the offset of retreat. All rasters have been sorted for movement duration. Response rasters contain approximately half as many trials as approach and retreat rasters (Table 3); y axis of PETH refers to average FR (spikes/second) per trial. Both x axes refer to time (msec).

during cocaine-seeking behavior (Ghitza et al., 2004, 2006; Hollander and Carelli, 2005; Fabbricatore et al., 2010), the NAcc core–VPdl subcircuit may be an especially important contributor to the approach and response components of cocaine self-administration.

The *patterns* in which changes in FR occurred also differed by subregion. The increases/decreases in FR during approach and response of VPdl neurons exhibited a significantly larger correlation coefficient than VPvm neurons, indicating that VPdl neurons were more rigid in their approach and response firing patterns. That is, changes in FR by VPdl neurons typically began during the approach and carried through the response in the same direction with similar or greater magnitude. In contrast, VPvm neurons were heterogeneous, changing FRs during the approach alone, response alone, or both approach

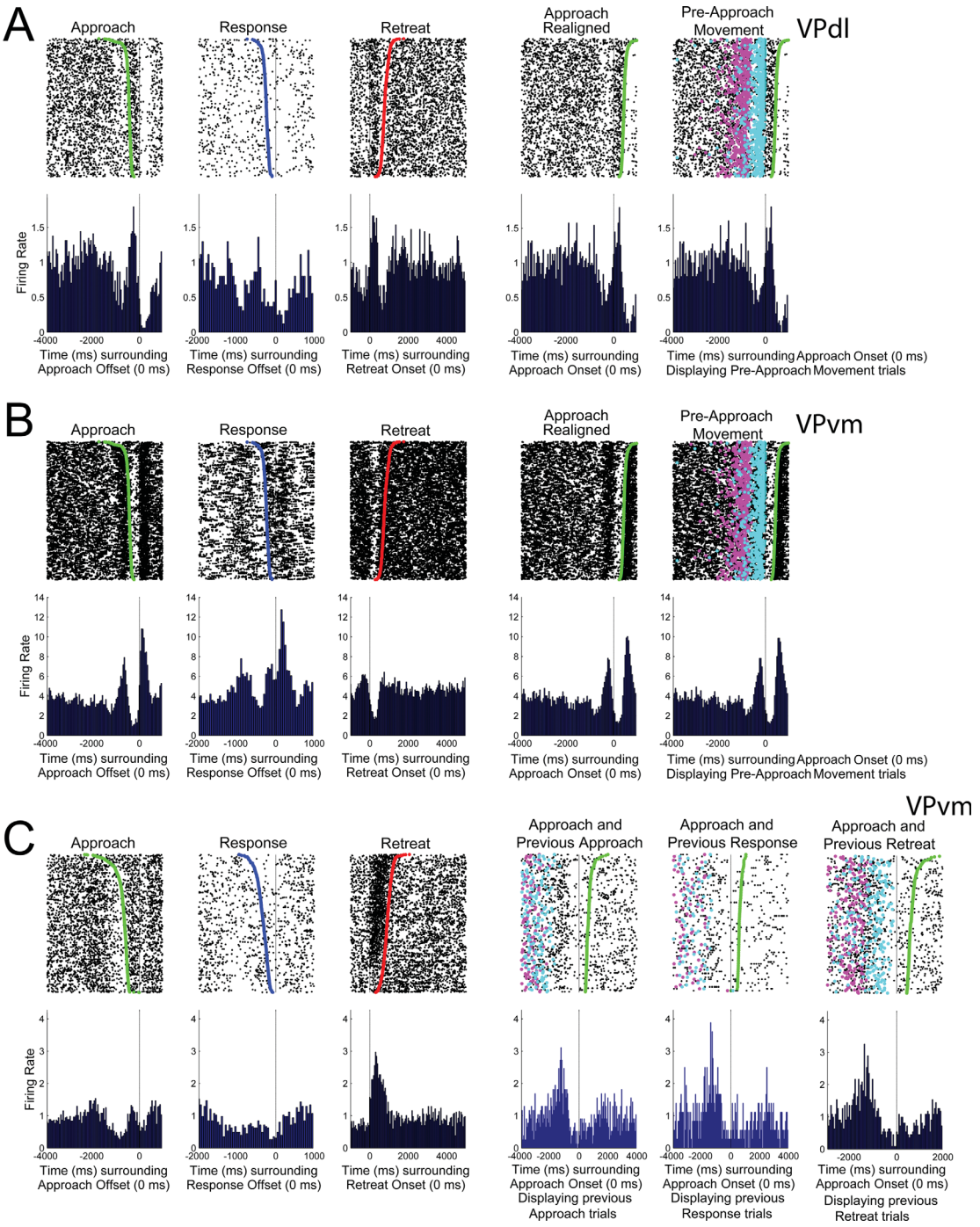

Figure 13 (legend on page 582).

and response. Taken together with the greater magnitude change in FR during approach and response by VPdl neurons compared with VPvm neurons, distinct firing patterns during these behaviors suggest that VP subregions play differential roles during drug-seeking behavior.

The VPdl, with weak projections to MDT and robust efferents to "motoric" regions such as subthalamic nucleus and medial substantia nigra pars reticulata (Groenewegen et al., 1993; Zahm et al., 1996), may be an important contributor to the expression of drug-seeking and drug-taking behaviors via its approach and response firing patterns. Fan et al. (2012) recently reported that many medial substantia nigra neurons (especially putative GABAergic neurons) exhibit changes in FR during responses. Our results suggest that the VPdl is one source of afferent input to substantia nigra pars reticulata neurons regulating changes in FR during the response. Furthermore, given that NAcc core neurons exhibited predominant increases in FR over NAcc shell neurons during cocaine-seeking (Ghitza et al., 2004) and that VPdl neurons were significantly decreased in FR compared with VPvm neurons during the response, the influence of VPdl GABAergic efferents on their targets during the response may be through disinhibition.

The VPvm exhibited heterogeneous firing patterns, including approach alone, response alone, and approach and response. The capacity of VPvm neurons to differentiate approach from response (i.e., drug-seeking from drug-taking) is consistent with greater convergent limbic signaling in the medial corticostriatopallidal circuit (French and Totterdell, 2002, 2003, 2004). Taken together with its robust innervation of the MDT and VTA (Zahm and Heimer, 1990; Groenewegen et al., 1993; Zahm et al., 1996; O'Donnell et al., 1997), heterogeneous firing patterns may implicate VPvm neurons in facilitating mesocortical structures with information related to different temporal components or sequences of behaviors that predict reward. In support, VP, MDT, and medial prefrontal cortex lesions disrupt performance following behavioral contingency changes (i.e., reversal learning or switching from Pavlovian to operant contingencies), in which monitoring of new appropriate behavioral sequences (approach, response, retreat) is critical (McBride and Slotnick, 1997; Ferry et al., 2000; Block et al., 2007; Pickens, 2008). Other firing patterns, also heterogeneous in direction, were observed in the VPvm more than in the VPdl, such as retreat alone and response-retreat. Such firing patterns may be involved in the association of cocaine-taking behaviors and their anticipated reinforcement. The NAcc shell, but not the core, supports intracranial self-administration of a variety of drugs of abuse (Carlezon et al., 1995; Carlezon and Wise, 1996a,b; Ikemoto et al., 1997, 2005; Rodd-Henricks et al., 2002; Shin et al., 2008), suggesting that the VPvm is involved in reward-related mechanisms.

In addition to heterogeneous firing patterns of shell neurons during cocaine self-administration (Ghitza et al., 2004; Fabbricatore et al., 2010), other factors may account for the heterogeneous directional changes in FR of VPvm neurons, such as the differential mean area densities of dopamine transporter- and tyrosine hydroxylase-labeled axons between VP subregions (Mengual and Pickel, 2004) or collaterals into VPvm from VPdl-projecting core neurons (Zahm and Brog, 1992; Brog et al., 1993; Tripathi et al., 2010). Additional sources of heterogeneity, which would affect both VP regions, may result

Figure 13. Absence of "initiation" firing patterns by VP neurons in the present task. Three candidate neurons are displayed, which were the only neurons that, upon first inspection, exhibited a potential firing pattern prior to the onset of approach (green dots in left panels of **A–C**). Blue dots and red dots in A–C indicate onset of response and offset of retreat, respectively. Time 0 (msec) in A–C (left) indicates offset of approach, time 0 (msec) in A–C (second from left) indicates offset of response, and time 0 (msec) in A–C (third from left) indicates onset of retreat. A (second from right) and B (second from right) are the same data from A (left) and B (left), respectively, except in A (second from right) and B (second from right) the onset of approach was redisplayed at time 0 and the *offset* of approach was displayed as green dots. Video analyses revealed that these neurons, recorded from the same animal, changed FRs during a locomotor movement prior to the approach rather than exhibiting an "initiation" (pre-movement) firing pattern (A, B see Supp. Info. Movie 2). In A (right) and B (right), magenta dots indicate the onset and cyan dots indicate offset of the pre-approach movement. For the neuron in C, the onset of approach was redisplayed at time 0 (msec) and offset of approach was indicated by green dots (first, second, and third panels from right). We examined whether changes in FR prior to the approach in C (left) were the result of approaches that were preceded within close proximity to other behaviors. C (third from right) displays trials in which a previous approach occurred within the 4-second firing window prior to the current approach. Prior approach onset and offset are displayed as magenta and cyan dots, respectively. C (second from right) displays trials in which a previous response occurred within the 4-second firing window prior to the approach. Prior response onset and offset are displayed as magenta and cyan dots, respectively. C (right) displays trials in which a previous retreat occurred within the 3-second firing window prior to the approach. Prior retreat onset and offset are displayed as magenta and cyan dots, respectively. This figure indicates that the decrease in FR observed in C (left) prior to the approach was due to a decrease in FR near the offset of the previous retreat, which was proximal to the approach onset (C (right). All rasters have been sorted for movement duration. Response rasters contain approximately half as many trials as approach and retreat rasters (Table 3); y axis of PETH refers to average FR (spikes/second) per trial. Both x axes refer to time (msec).

from chronic cocaine exposure, which alters GABA, opioid, and glutamate-induced changes in FR of VP neurons (McDaid et al., 2005); excitatory substance P projections from NAcc (Mitrovic and Napier, 1998), which rarely colocalize with GABAergic or enkephalinergic terminals in VP terminals (Zahm et al., 1985); and elevated extracellular dopamine or serotonin concentrations in VP during cocaine self-administration (Sizemore et al., 2000), which are robust modulators of VP FRs (Napier et al., 1991; Napier and Maslowski-Cobuzzi, 1994; Heidenreich and Napier, 2000). Whether the above manipulations differentially affect VP subregions is untested.

In primarily the VPvm, a small population of neurons exhibited changes in FR only during the retreat from the self-administration operandum. The absolute change in FR during the retreat did not differ between subregions. The retreat-related changes in FR observed here extend the "receptacle exit" firing patterns of NAcc neurons during natural reward-seeking behavior (Nicola et al., 2004a,b; Yun et al., 2004). It is likely that some retreat-related changes in FR reflect the "post-press" changes in FR (e.g., following response completion) observed in our previous examination of VP neurons using a lever press operant (Root et al., 2010). However, some firing patterns occurred after the retreat offset (Figs. 7B right, 10C right). Within each subregion, the directional change in FR during retreats involving pump onset significantly predicted the directional change in FR during retreats that did not contain pump onset, suggesting on the whole that the cocaine infusion did not induce a rapid phasic change in FR. The behaviorally relevant time scale for which our analyses occurred, hundreds of milliseconds (Table 3), is too rapid for pharmacologically induced changes in FR (discussed by Root et al., 2010). We have recognized pharmacological changes in FR by VP neurons in a previous report (Root et al., 2012), but these changes in FR occur over significantly longer time scales (minutes to hours). For the minority of neurons that exhibited differential firing patterns during pump vs. nonpump retreats, it is unclear whether retreats differ behaviorally between pump and nonpump conditions. Other factors, such as visceral effects of pump activation or potential success or error signals may contribute to firing patterns during the pump or nonpump retreat conditions. Furthermore, the retreat might reflect the anticipation of forthcoming cocaine reward and/or a behavior that leads to the onset of focused stereotypy. Further experimentation will be necessary to detail the factors involved in retreat-related firing patterns.

We observed no changes in FR related to S^D presentations. NAcc neurons exhibit a paucity of S^D-related changes in FR *during* cocaine self-administration (unpublished observations). One reason for the lack of changes in FR induced by the S^D may be that the S^D has little measurable behavioral influence while the animal is self-administering cocaine. During cocaine self-administration, responses occur only when the drug level falls below a unique individual internal threshold, above which the animal is satiated and does not respond (Pickens and Thompson, 1968; Wise, 1987; Lynch and Carroll, 2001; Norman and Tsibulsky, 2006). We have found evidence of such behavior using the same head movement paradigm employed in the present study. Specifically, clamping each animal's drug level immediately above its satiety threshold eliminated responding, whereas clamping drug level below satiety threshold markedly increased responding above baseline, irrespective of S^D presentations in both tests (Root et al., 2011). In other words, during cocaine self-administration, the animal's current drug level overshadows the influence of the S^D on behavior. Consistent with the inability of the S^D to guide behavior during self-administration, it is not surprising that VP neurons did not discriminate cued approaches from uncued approaches as well as cued responses from uncued responses. We suggest that changes in FR during approach and response are nevertheless "cue-induced" by the crossing of cocaine level below an internal threshold (Root et al., 2012) but not by the external S^D during self-administration. Whether VP neurons discriminate cued from uncued behaviors during natural reward seeking behavior, akin to NAcc neurons (Nicola et al., 2004a), is untested.

We and others observed no behavioral evidence that the S^D influences behavior during self-administration, but we have found that the animals nevertheless learn the relationship of S^D to the outcome of cocaine infusions. When the animal is abstinent, responding is low when the S^D is off and significantly increased following S^D presentation (Ghitza et al., 2003; Root et al., 2009). Furthermore, at this time when the S^D is behaviorally relevant (abstinent testing), NAcc neurons exhibit robust changes in FR following S^D presentation (Ghitza et al., 2003). Whether VP neurons show S^D-induced changes in FR during abstinence remains to be investigated.

The ventral striatopallidal system is hypothesized to be involved in goal-directed behaviors (Mogenson et al., 1980; Alexander et al., 1986). During cocaine self-administration, the same NAcc neurons that changed FR during approach and response did not exhibit changes in FR during locomotion induced by a treadmill (Chang et al., 1994), demonstrating "goal-directed" rather than "locomotor" firing patterns. Although the present study did not utilize a treadmill, we argue that the changes in FR observed in VP neurons were also goal directed. Given that 1) 66.67% of VPdl and 53.22% of VPvm neuron firing patterns included the response, 2) the response in the

present vertical head movement operant task precluded locomotion, and 3) no VP neurons exhibited significant correlations between FR and any motoric parameter of the response (e.g., distance, duration, velocity, valley, apex), other factors must be involved in producing the observed VP firing patterns during approach, response, and retreat. Furthermore, the lack of strictly "motoric" or "locomotor" firing correlates by VP neurons extends similar results from other laboratories. Mitchell and colleagues (1987) reported that VP neurons 1) exhibit no changes in FR in response to passive or active movement of any body part prior to conditioning and 2) do not encode information regarding direction and muscle pattern of movements following conditioning. Tindell and colleagues (2004) reported that VP neurons do not exhibit changes in FR during right and left stepping movements, i.e., locomotion.

The NAcc is the primary afferent of the VP (Zahm et al., 1985). Presumably, the goal-directed firing patterns observed in NAcc (Chang et al., 1994) are projected to the VP. Based on their groundbreaking studies of changes in FR during specific body part movements that occurred in serial fashion across interconnected regions of the "skeletomotor" dorsolateral striatal system, Alexander and colleagues (1986) predicted that firing patterns were similarly serially transmitted within the "cingulate" system; consisting of cortical projections to NAcc, followed by NAcc projections to VP, and subsequent VP projections to MDT. Seminal studies by Woodward and colleagues, recording medial prefrontal cortex (Chang et al., 1997, 2000) and NAcc (Chang et al., 1994, 2000) neurons during cocaine self-administration, together with the current VP study, provide critical insight into the function of this circuit. In the Chang et al. studies, the lever was positioned such that, in order to respond, rats had to approach the lever, rear, and position their forelimbs to press the lever downward. Firing patterns observed in their recordings of mPFC and NAcc were related exclusively to approaching the lever alone or to aspects involving the approach to the lever (rearing) and responding (touching the lever). Given that the most common firing patterns observed within the VP were related to approaching or responding alone on the operandum as well as approaching and responding together, the present results support the hypothesis (Alexander et al., 1986) of a maintained afferent firing pattern involving approach and response within the cingulate circuit. Given these arguments and the similar firing patterns observed between the present experiment utilizing a vertical head movement operant and our prior investigation of VP firing patterns using a different motoric requirement for cocaine self-infusions (lever press operant; Root et al., 2010), VP neurons appear to acquire firing patterns with one or more learned goal-directed behaviors involved in self-administering cocaine, regardless of motoric detail per se.

Whether VP passively relays signals from NAcc is not clear. The NAcc projects GABA to VP (Haber and Nauta, 1983; Zahm et al., 1985). However, the projection is predominantly opioid colocalized (Zahm et al., 1985; Olive et al., 1997), which is antagonistic to the effects of GABA (Chrobak and Napier, 1993). Other NAcc projections to VP contain substance P (Haber and Nauta, 1983; Zahm et al., 1985; Napier et al., 1995), which is excitatory on VP neurons (Napier et al., 1995; Mitrovic and Napier, 1998). With respect to cocaine-seeking behaviors, it appears that the VP (especially the VPvm) is more directionally heterogeneous in its firing patterns than NAcc neurons. We can only speculate that the signals from NAcc reach VP with additional heterogeneity because of colocalization and influences from other afferents. Our data do not resolve the mechanisms by which signals are processed within ventral striatopallidal pathways, and future research will be necessary.

Differences were observed between the present experiment and those reported by Tindell and colleagues (2004). The lack of cue-induced changes in FR observed in the present experiment but reported by Tindell et al. (2004) during a Pavlovian sucrose task likely was due to the cocaine self-administration paradigm (explained above). However, Tindell and colleagues (2004) also reported that only 3.03% (3/66) of VP neurons that exhibited CS^{+} or CS^{-}-related activity also exhibited a change in FR related to approaching the reward receptacle. Several reasons may explain this discrepancy. First, in contrast to the experiment of Tindell et al. (2004), the present experiment utilized immunohistochemistry as well as organized arrays of microwires rather than bundled electrodes. The present methods unequivocally localized every microwire recording reported in the present experiment to within the VP. Although VP is predominantly a subcommissural structure (Heimer and Wilson, 1975; Heimer, 1978; Heimer et al., 1997), the "hedonic hotspot" recordings from the Berridge/Aldridge laboratories (Tindell et al., 2004, 2005, 2006; Smith et al., 2011) tend to be located within the caudal, sublenticular parts of VP. Zahm and colleagues (2012) recently noted that the "hedonic 'hotspot' said to be located in the posterior part of the ventral pallidum may actually significantly involve the lateral preoptic area or a transitional merging of the ventral pallidum and lateral preoptic area." Thus, histological location of recorded neurons may be one reason for the differences between the present study and those from the Berridge/Aldridge laboratories. Second, NAcc neurons, the primary afferent of VP neurons, exhibit changes in FR during approach/response or "pre-response" epochs using cued (S^{D} or Pavlovian) as well as

uncued natural reward paradigms (Carelli and Deadwyler, 1994; Carelli et al., 2000; Chang et al., 2002; Nicola et al., 2004a,b; Yun et al., 2004; Wood et al., 2004; Day et al., 2006; Jones et al., 2010). This suggests that VP neurons would exhibit approach/response-related firing patterns, as we verify in the present report during cocaine self-administration, but it is plausible that differential firing patterns occur within VP neurons depending on the interaction of reward contingency (Pavlovian or Skinnerian) and type of reward (natural or drug reward).

Finally, of critical importance for drug-abuse research is the determination of which brain regions are responsible for initiating and executing drug-seeking behaviors. Mogenson and colleagues (1980) theorized that, through projections to the pedunculopontine tegmental mesencephalic locomotor region, VP provided a gateway for limbic/emotional signals sent to NAcc gain access to the motor system. If VP signals the initiation (Mogenson et al., 1980) of motivated behavior, one would expect firing pattern changes prior to the onset of approach. Only three candidate VP neurons exhibited changes in FR prior to the approach, which upon further inspection were revealed to be due to factors other than an initiation of firing correlate. Instead of preceding the onset of approach, VP FR changes in every case were coincident with approach, response, and/or retreat behaviors. Taken together with the arguments of Heimer and colleagues (1997), who contended that previous investigations of VP projections to the mesencephalic locomotor region "lumped" the VP with the subpallidal parts of the extended amygdala, VP is not likely the initiator of cocaine-seeking behavior. Instead, the role of VP in cocaine self-administration behaviors is subregionally dependent. The stronger, sustained FR changes of VPdl neurons during approach and response may implicate VPdl in similarly processing the acts of drug-seeking and drug-taking behaviors via projections to subthalamic nucleus and substantia nigra pars reticulata. In contrast, heterogeneous firing patterns of VPvm neurons may provide mesocortical structures with information related to the sequence of behaviors predicting cocaine self-infusions via projections to MDT and VTA. Thus, the present results provide a neurophysiological basis for functionally distinct but integrative involvement of VPdl and VPvm subregions in addiction.

ROLE OF AUTHORS

All authors had full access to all the data in the study and take responsibility for the integrity of the data and the accuracy of the data analysis. Study concept and design: DHR, ATF, MOW. Acquisition of data: DHR, LM, BMS, CMR. Statistical analysis and interpretation of the data: DHR, SM, DJB, MOW. Drafting of the manuscript: DHR, DJB, SM. Critical revision of the manuscript for important intellectual content: DHR, ATF, MOW. Obtained funding: DHR, DJB, MOW. Study supervision: ATF, MOW.

ACKNOWLEDGMENTS

This research served as partial fulfillment of the requirements for the degree of Doctor of Philosophy in the graduate program in Psychology at Rutgers, The State University of New Jersey, to D.H.R. We thank Drs. Laszlo Zaborszky, Alexander Kusnecov, and Elizabeth Torres for their insightful comments on a previous version of the manuscript. We thank Thomas Grace Sr., Anthony P. Pawlak, and Kevin R. Coffey for technical assistance. This article is dedicated to the memory of our friend and colleague Linda King (1950–2011). This research, along with the research from hundreds of graduate and undergraduate students over 23 years of dedication, depended on her scientific skills, insights, and instruction.

CONFLICT OF INTEREST STATEMENT

There are no conflicts of interest to disclose.

LITERATURE CITED

Ahmed SH, Koob GF. 1998. Transition from moderate to excessive drug intake: change in hedonic set point. Science 282:298–300.

Alexander GE, DeLong MR, Strick PL. 1986. Parallel organization of functionally segregated circuits linking basal ganglia and cortex. Annu Rev Neurosci 9:357–381.

Bell CC, Meek J, Yang JJ. 2005. Immunocytochemical identification of cell types in the mormyrid electrosensory lobe. J Comp Neurol 483:124–142.

Bell K, Churchill L, Kalivas PW. 1995. GABAergic projection from the ventral pallidum and globus pallidus to the subthalamic nucleus. Synapse 20:10–18.

Block AE, Dhanji H, Thompson-Tardif SF, Floresco SB. 2007. Thalamic-prefrontal cortical-ventral striatal circuitry mediates dissociable components of strategy set shifting. Cereb Cortex 17:1625–1636.

Bouilleret V, Loup F, Kiener T, Marescaux C, Fritschy JM. 2000. Early loss of interneurons and delayed subunit-specific changes in $GABA_A$-receptor expression in a mouse model of mesial temporal lobe epilepsy. Hippocampus 10: 305–324.

Brog JS, Salyapongse A, Deutch AY, Zahm DS. 1993. The patterns of afferent innervation of the core and shell in the "accumbens" part of the rat ventral striatum: immunohistochemical detection of retrogradely transported fluoro-gold. J Comp Neurol 338:255–278.

Buchan AMJ, Bambridge KG. 1988. Distribution and co-localization of calbindin D28k with VIP and neuropeptide Y but not somatostatin, galanin and substance P in the enteric nervous system of the rat. Peptides 9:333–338.

Cantwell EL, Cassone VM. 2006. Chicken suprachiasmatic nuclei: II. Autoradiographic and immunohistochemical analysis. J Comp Neurol 499:442–457.

Carelli RM, Deadwyler SA. 1994. A comparison of nucleus accumbens neuronal firing patterns during cocaine self-administration and water reinforcement in rats. J Neurosci 14:7735–7746.

Carelli RM, Ijames SG, Crumling AJ. 2000. Evidence that separate neural circuits in the nucleus accumbens encode cocaine vs. "natural" (water and food) reward. J Neurosci 20: 4255–4266.

Carlezon WA Jr, Wise RA. 1996a. Microinjections of phencyclidine (PCP) and related drugs into nucleus accumbens shell potentiate medial forebrain bundle brain stimulation reward. Psychopharmacology 128:413–420.

Carlezon WA Jr, Wise RA. 1996b. Rewarding actions of phencyclidine and related drugs in nucleus accumbens shell and frontal cortex. J Neurosci 16:3112–3122.

Carlezon WA Jr, Devine DP, Wise RA. 1995. Habit-forming actions of nomifensine in nucleus accumbens. Psychopharmacology 122:194–197.

Chang JY, Sawyer SF, Lee RS, Woodward DJ. 1994. Electrophysiological and pharmacological evidence for the role of the nucleus accumbens in cocaine self-administration in freely moving rats. J Neurosci 14:1224–1244.

Chang JY, Sawyer SF, Paris JM, Kirillov A, Woodward DJ. 1997. Single neuronal responses in medial prefrontal cortex during cocaine self-administration in freely moving rats. Synapse 26:22–35, 1997.

Chang JY, Janak PH, Woodward DJ. 2000. Neuronal and behavioral correlations in the medial prefrontal cortex and nucleus accumbens during cocaine self-administration by rats. Neuroscience 99:433–443.

Chang JY, Chen L, Luo F, Shi LH, Woodward DJ. 2002. Neuronal responses in the frontal cortico-basal ganglia system during delayed matching-to-sample task: ensemble recording in freely moving rats. Exp Brain Res 142:67–80.

Chrobak JJ, Napier TC. 1993. Opioid and GABA modulation of accumbens-evoked ventral pallidal activity. J Neural Transm 93:123–143.

Churchill L, Zahm DS, Kalivas PW. 1996. The mediodorsal nucleus of the thalamus in rats–I. forebrain gabaergic innervation. Neuroscience 70:83–102.

Conde F, Lund JS, Jacobowitz DM, Baimbridge KG, Lewis DA. 1994. Local circuit neurons immunoreactive for calretinin, calbindin d-28k or parvalbumin in monkey prefrontal cortex: distribution and morphology. J Comp Neurol 341: 95–116.

Dallimore JE, Mickiewicz AL, Napier TC. 2006. Intra-ventral pallidal glutamate antagonists block expression of morphine-induced place preference. Behav Neurosci 120: 1103–1114.

Day JJ, Wheeler RA, Roitman MF, Carelli RM. 2006. Nucleus accumbens neurons encode Pavlovian approach behaviors: evidence from an autoshaping paradigm. Eur J Neurosci 23:1341–1351.

Deroche-Gamonet V, Belin D, Piazza PV. 2004. Evidence for addiction-like behavior in the rat. Science 305:1014–1017.

Eggerman KW, Zahm DS. 1988. Numbers of neurotensin-immunoreactive neurons selectively increased in rat ventral striatum following acute haloperidol administration. Neuropeptides 11:125–132.

Fabbricatore AT, Ghitza UE, Prokopenko VF, West MO. 2010. Electrophysiological evidence of mediolateral functional dichotomy in the rat nucleus accumbens during cocaine self-administration II: phasic firing patterns. Eur J Neurosci 31:1671–1682.

Fan D, Rossi MA, Yin HH. 2012. Mechanisms of action selection and timing in substantia nigra neurons. J Neurosci 32: 5534–5548.

Ferry AT, Lu XC, Price JL. 2000. Effects of excitotoxic lesions in the ventral striatopallidal–thalamocortical pathway on odor reversal learning: inability to extinguish an incorrect response. Exp Brain Res 131:320–335.

Fowler SC, Birkenstrand B, Chen R, Vorontsova E, Zarcone T. 2003. Behavioral sensitization toamphetamine in rats: changes in the rhythm of head movements during focused stereotypies. Psychopharmacology 170:167–177.

Fowler SC, Covington HE, Miczek KA. 2007. Stereotyped and complex motor routines expressed during cocaine self-administration: results from a 24-h binge of unlimited cocaine access in rats. Psychopharmacology 192:465–478.

Frankel PS, Alburges ME, Bush L, Hanson GR, Kish SJ. 2008. Striatal and ventral pallidum dynorphin concentrations are markedly increased in human chronic cocaine users. Neuropharmacology 55:41–46.

French SJ, Totterdell S. 2002. Hippocampal and prefrontal cortical inputs monosynaptically converge with individual projection neurons of the nucleus accumbens. J Comp Neurol 446:151–165.

French SJ, Totterdell S. 2003. Individual nucleus accumbens-projection neurons receive both basolateral amygdala and ventral subicular afferents in rats. Neuroscience 119: 19–31.

French SJ, Totterdell S. 2004. Quantification of morphological differences in boutons from different afferent populations to the nucleus accumbens. Brain Res 1007:167–177.

Geisler S, Zahm DS. 2006a. Neurotensin afferents of the ventral tegmental area in the rat: [1] re-examination of their origins and [2] responses to acute psychostimulant and antipsychotic drug administration. Eur J Neurosci 24: 116–134.

Geisler S, Zahm DS. 2006b. On the retention of neurotensin in the ventral tegmental area (VTA) despite destruction of the main neurotensinergic afferents of the VTA–implications for the organization of forebrain projections to the VTA. Brain Res 1087:87–104.

Ghitza UE, Fabbricatore AT, Prokopenko V, Pawlak AP, West MO. 2003. Persistent cue-evoked activity of accumbens neurons after prolonged abstinence from self-administered cocaine. J Neurosci 23:7239–7245.

Ghitza UE, Fabbricatore AT, Prokopenko VF, West MO. 2004. Differences between accumbens core and shell neurons exhibiting phasic firing patterns related to drug-seeking behavior during a discriminative stimulus task. J Neurophysiol 92:1608–1614.

Ghitza UE, Prokopenko VF, West MO, Fabbricatore AT. 2006. Higher magnitude accumbal phasic firing changes among core neurons exhibiting tonic firing increases during cocaine self-administration. Neuroscience 137:1075–1085.

Gong W, Neill D, Justice JB Jr. 1997. 6-Hydroxydopamine lesion of ventral pallidum blocks acquisition of place preference conditioning to cocaine. Brain Res 754:103–112.

Groenewegen HJ, Berendse HW, Haber SN. 1993. Organization of the output of the ventral striatopallidal system in the rat: ventral pallidal efferents. Neuroscience 57: 113–142.

Groenewegen HJ, Russchen FT. 1984. Organization of the efferent projections of the nucleus accumbens to pallidal, hypothalamic, and mesencephalic structures: a tracing and immunohistochemical study in the cat. J Comp Neurol 223:347–367.

Haber SN, Groenewegen HJ, Grove EA, Nauta WJ. 1985. Efferent connections of the ventral pallidum: evidence of a dual striato pallidofugal pathway. J Comp Neurol 235:322–335.

Haber SN, Nauta WJ. 1983. Ramifications of the globus pallidus in the rat as indicated by patterns of immunohistochemistry. Neuroscience 9:245–260.

Heidenreich BA, Napier TC. 2000. Effects of serotonergic 5-HT1A and 5-HT1B ligands on ventral pallidal neuronal activity. Neuroreport 11:2849–2853.

Heimer L. 1978.The olfactory cortex and the ventral striatum. In:Livingston KE,Hornykiewicz O, editors. Limbic mechanisms. New York: Plenum Press. p 95–188.

Heimer L, Wilson RD. 1975.The subcortical projections of the allocortex: similarities in the neural associations of the hippocampus, the piriform cortex, and the neocortex. In:Santini M, editor. Golgi centennial symposium. New York: Raven Press. p177–193.

Heimer L, Zahm DS, Churchill L, Kalivas PW,Wohltmann. 1991. Specificity in the projection patterns of accumbal core and shell in the rat. Neuroscience 41:89–125.

Heimer L, Harlan RE, Alheid GF, Garcia MM, de Olmos J. 1997. Substantia innominata: a notion which impedes clinical–anatomical correlations in neuropsychiatric disorders. Neuroscience 76:957–1006.

Hollander JA, Carelli RM. 2005. Abstinence from cocaine self-administration heightens neural encoding of goal-directed behaviors in the accumbens. Neuropsychopharmacology 30:146–1474.

Ikemoto S, Glazier BS, Murphy JM, McBride WJ. 1997. Role of dopamine D1 and D2 receptors in the nucleus accumbens in mediating reward. J Neurosci 17:8580–8587.

Ikemoto S, Qin M, Liu ZH. 2005. The functional divide for primary reinforcement of D-amphetamine lies between the medial and lateral ventral striatum: is the division of the accumbens core, shell, and olfactory tubercle valid? J Neurosci 25:5061–5065.

Johnson PI, Napier TC. 2000. Ventral pallidal injections of a mu antagonist block the development of behavioral sensitization to systemic morphine. Synapse 38:61–70.

Jones JL, Day JJ, Wheeler RA, Carelli RM. 2010. The basolateral amygdala differentially regulates conditioned neural responses within the nucleus accumbens core and shell. Neuroscience 169:1186–1198.

Kalivas PW, Churchill L, Klitenick MA. 1993. GABA and enkephalin projection from the nucleus accumbens and ventral pallidum to the ventral tegmental area. Neuroscience 57:1047–1060.

Kim YS, Paik SK, Cho YS, Shin HS, Bae JY, Moritani M, Yoshida A, Ahn DK, Valtschanoff J, Hwang SJ, Moon C, Bae YC. 2008. Expression of p2x3 receptor in the rat trigeminal sensory nuclei of the rat. J Comp Neurol 506:627–639.

Kuo H, Chang HT. 1992. Ventral pallido-striatal pathway in the rat brain: a light and electron microscopic study. J Comp Neurol 321:626–36.

Kuroda M, Price JL. 1991. Synaptic organization of projections from basal forebrain structures to the mediodorsal thalamic nucleus of the rat. J Comp Neurol 303:513–533.

Lynch WJ, Carroll ME. 2001. Regulation of drug intake. Exp Clin Psychopharmacol 9:131–143.

Ma S. 2010. Raster and PETH Simple Version. Retrieved from http://www.mathworks.com/matlabcentral/fileexchange/29763-raster-and-peth-simple-version.

McBride SA, Slotnick B. 1997. The olfactory thalamocortical system and odor reversal learning examined using an asymmetrical lesion paradigm in rats. Behav Neuorsci 111: 1273–1284.

McDaid J, Dallimore JE, Mackie AR, Mickiewicz AL, Napier TC. 2005. Cross-sensitization to morphine in cocaine-sensitized rats: behavioral assessments correlate with enhanced responding of ventral pallidal neurons to morphine and glutamate, with diminished effects of GABA. J Pharmacol Exp Ther 313:1182–1193.

McFarland K, Kalivas PW. 2001. The circuitry mediating cocaine-induced reinstatement of drug-seeking behavior. J Neurosci 21:8655–8663.

McFarland K, Davidge SB, Lapish CC, Kalivas PW. 2004. Limbic and motor circuitry underlying footshock-induced reinstatement of cocaine-seeking behavior. J Neurosci 24: 1551–1560.

Meek J, Yang JJ, Han VZ, Bell CC. 2008. Morphological analysis of the mormyrid cerebellum using immunohistochemistry with emphasis on the unusual neuronal organization of the valvula. J Comp Neurol 510:396–421.

Mengual E, Pickel VM. 2004. Regional and subcellular compartmentation of the dopamine transporter and tyrosine hydroxylase in the rat ventral pallidum. J Comp Neurol 468:395–409.

Mickiewicz AL, Dallimore JE, Napier TC. 2009. The ventral pallidum is critically involved in the development and expression of morphine-induced sensitization. Neuropsychopharmacology 34:874–886.

Mitchell SJ, Richardson RT, Baker FH, DeLong MR. 1987. The primate globus pallidus: neuronal activity related to direction of movement. Exp Brain Res 68:491–505.

Mitrovic I, Napier TC. 1998. Substance P attenuates and DAMGO potentiates amygdala glutamatergic neurotransmission within the ventral pallidum. Brain Res 792:193–206.

Mogenson GJ, Jones DL, Yim CY. 1980. From motivation to action: functional interface between the limbic system and the motor system. Prog Neurobiol 14:69–97.

Morse DT. 1999. MINSIZE2: a computer program for determining effect size and minimum sample size for statistical significance for univariate, multivariate, and nonparametric tests. Educ Psychol Meas 59:518–531.

Napier TC, Maslowski-Cobuzzi RJ. 1994. Electrophysiological verification of the presence of D1 and D2 dopamine receptors within the ventral pallidum. Synapse 17:160–166.

Napier TC, Simson PE, Givens BS. 1991. Dopamine electrophysiology of ventral pallidal/substantia innominata neurons: comparison with the dorsal globus pallidus. J Pharmacol Exp Ther 258:249–262.

Napier TC, Mitrovic I, Churchill L, Klitenick MA, Lu XY, Kalivas PW. 1995. Substance P in the ventral pallidum: projection from the ventral striatum, and electrophysiological and behavioral consequences of pallidal substance P. Neuroscience 69:59–70.

Nicola SM, Yun IA, Wakabayashi KT, Field HL. 2004a. Firing of nucleus accumbens neurons during the consummatory phase of a discriminative stimulus task depends on previous reward predictive cues. J Neurophysiol 91:1866–1882.

Nicola SM, Yun IA.Wakabayashi KY, Fields HL. 2004b. Cue-evoked firing of nucleus accumbens neurons encodes motivational significance during a discriminative stimulus task. J Neurophysiol 91:1840–1865.

Norman AB, Tsibulsky VL. 2006. The compulsion zone: a pharmacological theory of acquired cocaine self-administration. Brain Res 1116:143–152.

O'Donnell P, Lavín A, Enquist LW, Grace AA, Card JP. 1997. Interconnected parallel circuits between rat nucleus accumbens and thalamus revealed by retrograde transynaptic transport of pseudorabies virus. J Neurosci 17:2143–2167.

Olive MF, Anton B, Micevych P, Evans CJ, Maidment NT. 1997. Presynaptic vs. postsynaptic localization of m and d opioid receptors in dorsal and ventral striatopallidal pathways. J Neurosci 17:7471–7479.

Pawlak AP, Tang CC, Pederson C, Wolske MB, West MO. 2010. Acute effects of cocaine on movement-related firing of dorsolateral striatal neurons depend on predrug firing rate and dose. J Pharmacol Exp Ther 332:667–683.

Paxinos G, Watson C. 1997. The rat brain in stereotaxic coordinates. Third Edition. New York: Academic Press.

Paxinos G, Watson C. 2005. The rat brain in stereotaxic coordinates. Fifth Edition. New York: Academic Press.

Pederson CL, Wolske M, Peoples LL, West MO. 1997. Firing rate dependent effect of cocaine on firing of single neurons in the rat lateral striatum. Brain Res 760:261–265.

Pickens CL. 2008. A limited role for mediodorsal thalamus in devaluation tasks. Behav Neurosci 122:659–676.

Pickens R, Thompson T. 1968. Cocaine-reinforced behavior in rats: effects of reinforcement magnitude and fixed-ratio size. J Pharmacol Exp Ther 161:122–129.

Rademacher DJ, Kovacs B, Shen F, Napier TC, Meredith GE. 2006. The neural substrates of amphetamine conditioned place preference: implications for the formation of conditioned stimulus–reward associations. Eur J Neurosci 24: 2089–2097.

Riedel A, Härtig W, Seeger G, Gärtner U, Brauer K, Arendt T. 2002. Principles of rat subcortical forebrain organization: a study using histological techniques and multiple fluorescence labeling. J Chem Neuroanat 23:75–104.

Robledo P, Koob GF. 1993. Two discrete nucleus accumbens projection areas differentially mediate cocaine self-administration in the rat. Behav Brain Res 55:159–166.

Rodd-Henricks ZA, McKinzie DL, Li TK, Murphy JM, McBride WJ. 2002. Cocaine is self-administered into the shell but not the core of the nucleus accumbens ofz Wistar rats. J Pharmacol Exp Ther 303:1216–1226.

Root DH, Fabbricatore AT, Barker DJ, Ma S, Pawlak AP, West MO. 2009. Evidence for habitual and goal-directed behavior following devaluation of cocaine: a multifaceted interpretation of relapse. PLoS One 4:e7170.

Root DH, Fabbricatore AT, Ma S, Barker DJ, West MO. 2010. Rapid phasic activity of ventral pallidal neurons during cocaine self-administration. Synapse 64:704–713.

Root DH, Barker DJ, Ma S, Coffee KR, Fabbricatore AT, West MO. 2011. Evidence for skilled cocaine self-administration in rats. Psychopharmacology 217:91–100.

Root DH, Fabbricatore AT, Pawlak AP, Barker DJ, Ma S, West MO. 2012. Slow phasic and tonic activity of ventral pallidal neurons during cocaine self-administration. Synapse 66:106–127.

Shin R, Qin M, Liu ZH, Ikemoto S. 2008. Intracranial self-administration of MDMA into the ventral striatum of the rat: differential roles of the nucleus accumbens shell, core, and olfactory tubercle. Psychopharmacology 198: 261–270.

Sizemore GM, Co C, Smith JE. 2000. Ventral pallidal extracellular fluid levels of dopamine, serotonin, gamma amino butyric acid, and glutamate during cocaine self-administration in rats. Psychopharmacology 150:391–398.

Smith KS, Berridge KC, Aldridge JW. 2011. Disentangling pleasure from incentive salience and learning signals in brain reward circuitry. Proc Natl Acad Sci U S A 108: E255–E264.

Taha SA, Fields HL. 2006. Inhibitions of nucleus accumbens neurons encode a gating signal for reward-directed behavior. J Neurosci 26:217–222.

Tang C, Pawlak AP, Prokopenko V, West MO. 2007. Changes in activity of the striatum during formation of a motor habit. Eur J Neurocsi 25:1212–1227.

Tang XC, McFarland K, Cagle S, Kalivas PW. 2005. Cocaine-induced reinstatement requires endogenous stimulation of mu-opioid receptors in the ventral pallidum. J Neurosci 25: 4512–4520.

Tiffany ST. 1990. A cognitive model of drug urges and drug-use behavior: role of automatic and nonautomatic processes. Psychol Rev 97:147–168.

Tindell AJ, Berridge KC, Aldridge JW. 2004. Ventral pallidal representation of pavlovian cues and reward: population and rate codes. J Neurosci 24:1058–1069.

Tindell AJ, Berridge KC, Zhang J, Peciña S, Aldridge JW. 2005. Ventral pallidal neurons code incentive motivation: amplification by mesolimbic sensitization and amphetamine. Eur J Neurosci 22:2617–2634.

Tindell AJ, Smith KS, Peciña S, Berridge KC, Aldridge JW. 2006. Ventral pallidum firing codes hedonic reward: when a bad taste turns good. J Neurophysiol 96:2399–2409.

Tripathi A, Prensa L, Cebrian C, Mengual E. 2010. Axonal branching patterns of nucleus accumbens neurons in rat. J Comp Neurol 518:4649–4673.

Weissner W, Winterson BJ, Stuart-Tilley A, Devor M, Bove GM. 2006. Time course of substance p expression in dorsal root ganglia following complete spinal nerve transection. J Comp Neurol 497:78–87.

Wise RA. 1987.Intravenous drug self-administration: a special case of positive reinforcement. In:Bozarth MA, editor. Methods of assessing the reinforcing properties of abused drugs. New York: Springer. p117–141.

Wood DA, Kosobud AE, Rebec GV. 2004. Nucleus accumbens single-unit activity in freely behaving male rats during approach to novel and non-novel estrus. Neurosci Lett 368:29–32.

Yun IA, Wakabayashi KT, Fields HL, Nicola SM. 2004. The ventral tegmental area is required for the behavioral and nucleus accumbens neuronal firing responses to incentive cues. J Neurosci 24:2923–2933.

Zahm DS. 1989. The ventral striatopallidal parts of the basal ganglia in the rat–II. Compartmentation of ventral pallidal efferents. Neuroscience 30:33–50.

Zahm DS, Brog JS. 1992. On the significance of subterritories in the "accumbens" part of the rat ventral striatum. Neuroscience 50:751–767.

Zahm DS, Heimer L. 1988. Ventral striatopallidal parts of the basal ganglia in the rat: I. Neurochemical compartmentation as reflected by the distributions of neurotensin and substance p immunoreactivity. J Comp Neurol 272: 516–535.

Zahm DS, Heimer L. 1990. Two transpallidal pathways originating in the rat nucleus accumbens. J Comp Neurol 302: 437–446.

Zahm DS, Zaborszky L, Alones VE, Heimer L. 1985. Evidence for the coexistence of glutamate decarboxylase and met-enkephalin immunoreactivities in axon terminals of rat ventral pallidum. Brain Res 325:317–321.

Zahm DS, Williams E, Wohltmann C. 1996. Ventral striatopallidothalamic projection: IV. Relative involvements of neurochemically distinct subterritories in the ventral pallidum and adjacent parts of the rostroventral forebrain. J Comp Neurol 364:340–362.

Zahm DS, Cheng AY, Lee TJ, Ghobadi CW, Schwartz ZM, Geisler S, Parsely KP, Gruber C, Veh RW. 2011. Inputs to the midbrain dopaminergic complex in the rat, with emphasis on extended amygdala-recipient sectors. J Comp Neurol 519:3159–3188.

Zahm DS, Parsely KP, Schwartz ZM, Cheng AY. 2012. On lateral septum-like characteristics of outpute from the accumbal hedonic "hotspot" of Pecina and Berridge with commentary on the transitional nature of basal forebrain "boundaries." J Comp Neurol (in press).